Crustal structure of the ocean-continent transition at Flemish Cap: Seismic refraction results

Thomas Funck,[1] John R. Hopper,[1] Hans Christian Larsen,[1] Keith E. Louden,[2] Brian E. Tucholke,[3] and W. Steven Holbrook[4]

[1] We conducted a seismic refraction experiment across Flemish Cap and into the deep basin east of Newfoundland, Canada, and developed a velocity model for the crust and mantle from forward and inverse modeling of data from 25 ocean bottom seismometers and dense air gun shots. The continental crust at Flemish Cap is 30 km thick and is divided into three layers with P wave velocities of 6.0–6.7 km/s. Across the southeast Flemish Cap margin, the continental crust thins over a 90-km-wide zone to only 1.2 km. The ocean-continent boundary is near the base of Flemish Cap and is marked by a fault between thinned continental crust and 3-km-thick crust with velocities of 4.7–7.0 km/s interpreted as crust from magma-starved oceanic accretion. This thin crust continues seaward for 55 km and thins locally to ~1.5 km. Below a sediment cover (1.9–3.1 km/s), oceanic layer 2 (4.7–4.9 km/s) is ~1.5 km thick, while layer 3 (6.9 km/s) seems to disappear in the thinnest segment of the oceanic crust. At the seawardmost end of the line the crust thickens to ~6 km. Mantle with velocities of 7.6–8.0 km/s underlies both the thin continental and thin oceanic crust in an 80-km-wide zone. A gradual downward increase to normal mantle velocities is interpreted to reflect decreasing degree of serpentinization with depth. Normal mantle velocities of 8.0 km/s are observed ~6 km below basement. There are major differences compared to the conjugate Galicia Bank margin, which has a wide zone of extended continental crust, more faulting, and prominent detachment faults. Crust formed by seafloor spreading appears symmetric, however, with 30-km-wide zones of oceanic crust accreted on both margins beginning about 4.5 m.y. before formation of magnetic anomaly M0 (~118 Ma).   INDEX TERMS: 3025 Marine Geology and Geophysics: Marine seismics (0935); 8105 Tectonophysics: Continental margins and sedimentary basins (1212); 9325 Information Related to Geographic Region: Atlantic Ocean; KEYWORDS: refraction seismics, ocean-continent transition, serpentinized mantle

1. Introduction

[2] Rifted margins are created by extension and breakup of continental crust to form intervening ocean basins. They are often classified as volcanic or nonvolcanic based on the amount of extrusive and intrusive magmatic activity during the rifting [*Louden and Lau*, 2001]. The mechanical behavior of the lithosphere under extension is well studied on nonvolcanic margins where the extensional fabric has not been modified by large volumes of synrift or postrift volcanism. The best studied nonvolcanic margin is the Iberia margin, which was drilled at Galicia Bank during leg 103 of the Ocean Drilling Program (ODP) and in the Iberia Abyssal Plain during legs 149 and 173. The Iberia margin is characterized by the exhumation of continental mantle during the final stages of breakup. Shallow mantle rocks were then transformed to serpentinite by high-temperature interaction with seawater [*Sawyer et al.*, 1994; *Whitmarsh et al.*, 1996; *Discovery 215 Working Group*, 1998; *Whitmarsh et al.*, 2000]. The extreme lithospheric thinning was accompanied by little or no decompressional melting of the asthenospheric mantle, which poses a problem for melting models at rifted margins [*Minshull et al.*, 2001]. The width of the transition zone exhibiting serpentinized mantle varies along strike off Iberia, with a wider zone in the southern Iberia Abyssal Plain [*Dean et al.*, 2000] and a narrow zone off Galicia Bank [*Whitmarsh et al.*, 1996].

[3] The Newfoundland continental margin is conjugate to the Iberia margin (Figure 1) and geophysical studies indicate significant cross-rift asymmetries. Previous refraction seismic work on the Newfoundland margin is sparse, but

---

[1]Danish Lithosphere Centre, Copenhagen, Denmark.
[2]Department of Oceanography, Dalhousie University, Halifax, Nova Scotia, Canada.
[3]Department of Geology and Geophysics, Woods Hole Oceanographic Institution, Woods Hole, Massachusetts, USA.
[4]Department of Geology and Geophysics, University of Wyoming, Laramie, Wyoming, USA.
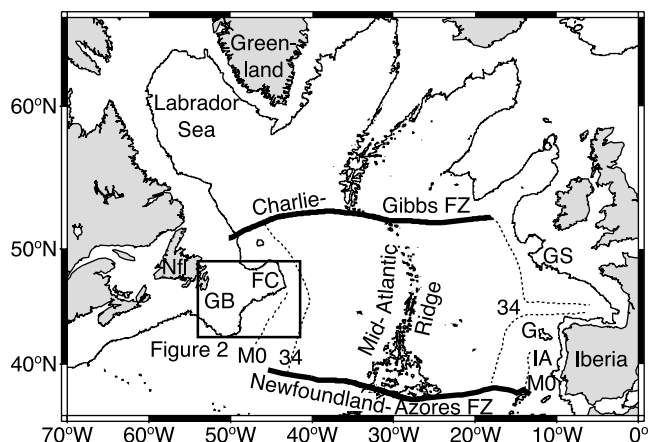
Figure 1. Location map of the conjugate Newfoundland and Iberia margins. Thin solid line shows the 2000-m bathymetric contour. Thick solid lines indicate fracture zones (FZ). Magnetic anomalies M0 and M34 are marked by dashed lines. Abbreviations are FC, Flemish Cap; GB, Grand Banks; Nfl, Newfoundland; G, Galicia Bank; IA, Iberia Abyssal Plain; GS, Goban Spur.

there is no indication of exhumed mantle in the transition zone between the extended continental crust and normal oceanic crust. However, there is evidence for serpentinized mantle underneath oceanic and thinned continental crust (*Reid*'s [1994] reinterpretation of *Todd and Reid* [1989]; *Louden and Chian*'s [1999] reinterpretation of *Reid and Keen* [1990]; *Reid* [1994]).

[4] Consistent data along both margin conjugates are necessary to understand the asymmetries and to advance the interpretation of existing data sets. Since the Newfoundland margin is not as well sampled as the Iberia counterpart, a reflection and refraction seismic study was initiated to improve the image of the crustal structure along the Newfoundland margin. The experiment was carried out in 2000 as part of the SCREECH (Study of Continental Rifting and Extension on the Eastern Canadian Shelf) project with three major transects (Figure 2). This paper presents the results of the northernmost refraction seismic line (line 1) across Flemish Cap. Record sections of the coincident reflection seismic line are shown by *Hopper et al.* [2003]. Line 1 is conjugate to the ODP drilling transect of leg 103 [*Boillot et al.*, 1987] and refraction line 6 [*Whitmarsh et al.*, 1996] on the Galicia Bank continental margin. More recent reflection and refraction seismic data from Galicia Bank and the Galicia Interior Basin are presented by *Pérez-Gussinyé et al.* [2003] and *Zelt et al.* [2003].
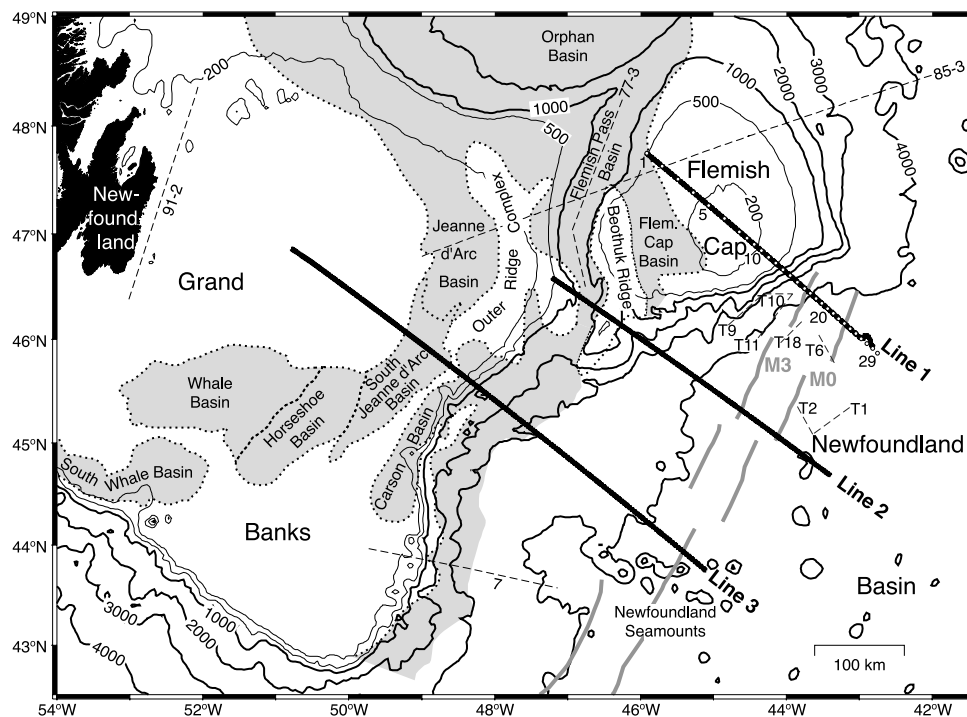
Figure 2. Bathymetric map of the study area showing the location of the three lines of the SCREECH experiment. Solid bold lines show the shot line. Circles along line 1 indicate the locations of ocean bottom seismographs (annotations show the station number). Contour interval of the bathymetry is 1000 m (solid lines). In addition, the 200- and 500-m-depth contours are plotted (thin solid lines). Rift basins on the Grand Banks and Flemish Cap (modified from *Grant and McAlpine* [1990]) are shown as shaded regions with dotted lines. Magnetic anomalies M0 and M3 (gray lines) are taken from *Srivastava et al.* [2000]. Seismic lines relevant to this study are shown by dashed lines: line 77-3 [*Keen and Barrett*, 1981]; line 85-3 [*Keen et al.*, 1987]; line 7 [*Reid*, 1994]; line 91-2 [*Marillier et al.*, 1994]; T1-18 [*Todd and Reid*, 1989].

[5] The new seismic data on the Newfoundland margin were collected to determine the exact character of the perceived asymmetry between the conjugate margins and the mechanisms that caused the deformation. Some of the key questions to be addressed by the SCREECH refraction seismic data include the following: (1) Is the continental mantle on the Newfoundland margin unroofed and serpentinized in a manner similar to that on the Iberia side? (2) What is the amount and distribution of crustal extension? (3) Is there any evidence for significant magmatism?

2. Geological Setting

[6] The Flemish Cap is a roughly circular fragment of continental crust located some 600 km east of Newfoundland (Figure 2). The crustal thickness has been estimated to be 28 km based on reflection seismic data [*Keen et al.*, 1987, 1989]. Flemish Cap consists of a central core of rocks of Hadrynian age (750–830 Ma), with an onlapping sequence of undisturbed to disturbed Mesozoic-Cenozoic sediments [*King et al.*, 1985]. Basement in the core zone consists mainly of weakly metamorphosed granodiorite or granite, and some volcanic rocks. *King et al.* [1985] concluded that Flemish Cap is part of the Avalon Zone of the Appalachian orogen.

[7] In the southwestern segment of Flemish Cap more than 3 km of sediments are present in a north trending half-graben basin bounded to the west by the Beothuk Ridge [*Grant and McAlpine*, 1990]. Sediments in this graben are probably of Early to Late Cretaceous age [*Grant and McAlpine*, 1990]. To the west, Flemish Cap is separated from the Grand Banks by the Flemish Pass rift basin. Moho depth at Flemish Pass is ∼22 km and the sediment infill is around 6 km [*Keen and Barrett*, 1981], indicating basement thickness of about 16 km.

[8] Rifting at the Newfoundland margin occurred in three major phases [*Tucholke et al.*, 1989; *Grant and McAlpine*, 1990]. During the first phase in the Late Triassic, northeast trending grabens on the Grand Banks were formed. The second phase of rifting began in the Late Jurassic and continued until the Grand Banks/Flemish Cap were separated from Iberia, with the rift propagating from south to north. According to the plate reconstruction of *Srivastava et al.* [2000], magnetic anomaly M3 (early Barremian, ∼126 Ma) is the oldest anomaly recognizable in the north at Flemish Cap. A third, Late Cretaceous phase of rifting led to the opening of Labrador Sea and the separation of Orphan Knoll and the northern part of Flemish Cap from NW Europe and Rockall Plateau. Seafloor spreading between northern Flemish Cap and Goban Spur (Figure 1) was initiated ∼110 Ma [*Srivastava et al.*, 1988].

3. Wide-Angle Seismic Experiment

3.1. Data Acquisition

[9] Line 1 of the SCREECH experiment is a 320-km-long NW-SE transect across Flemish Cap into Newfoundland Basin (Figure 2). The refraction/wide-angle reflection (R/WAR) seismic work along the line was a two-ship operation. Ocean bottom seismometer (OBS) operations were carried out by R/V *Oceanus*, while the air gun array was towed by R/V *Maurice Ewing*. The tuned array consisted of 20 air guns with a total volume of 140 L. Individual gun sizes ranged from 2.4 L to 14.3 L. The shot spacing was 200 m.

[10] 29 OBS were deployed along the transect. 14 instruments (owned by Dalhousie University and the Geological Survey of Canada) were equipped with three-component 4.5-Hz geophones and a hydrophone, while the other 15 recorders (owned by Woods Hole Oceanographic Institution) had a hydrophone component only. The station spacing varied from 21 km in the shallow water of Flemish Cap to 8 km in Newfoundland Basin. One instrument could not be recovered after the experiment (OBS 9), and three instruments did not record any data due to technical problems (OBS 1, 24, and 29).

[11] While the OBS were being recovered by R/V *Oceanus*, R/V *Maurice Ewing* shot the line a second time in order to collect coincident multichannel seismic (MCS) data [*Hopper et al.*, 2003]. Segments of these shots with a spacing of 50 m were recorded by some of the OBS.

[12] For navigation (OBS and shot locations) and shot timing, the Global Positioning System (GPS) was used. Water depths along the transect were obtained from the R/V *Maurice Ewing*'s Hydrosweep center beam using a depth-velocity function from a CTD (conductivity, temperature, depth) measurement at the southeast end of the transect down to a depth of 4300 m.

3.2. Data Processing

[13] OBS data were converted to SEGY format, and time corrections for the drift of the OBS clock were applied. Data were debiased and resampled to 10 ms. Travel times of the direct wave were used to determine the exact position of the OBS at the seafloor, from which the shot-receiver ranges were calculated. The maximum offset between OBS deployment position and location on the seafloor was 1350 m.

[14] Amplitude spectra show that the main seismic energy is in the frequency range from 5 to 10 Hz. The record sections were band-pass filtered from 4.5 to 11 Hz. Seven instruments were affected by 6-Hz noise of unknown origin on the geophone components. Some OBS recorded this noise continuously while other instruments were only periodically exposed to the signal. Seismic traces that were affected by the noise were notch filtered. To preserve the seismic energy, it was necessary to use steep filter slopes, which sometimes created ripples around the wavelet.

[15] The seismic data were also deconvolved to sharpen the wavelet and on some OBS an fk filter was applied to reduce steeply dipping coherent noise. Traces in the record sections in Figures 3–7 are weighted by their distance to the OBS to increase the amplitudes for large offsets.

3.3. Methodology

[16] Deployment positions of the OBS were located along a great circle arc, which defines the baseline for the two-dimensional velocity modeling. OBS 1 defines the origin of the horizontal axis ($x = 0$ km) and the southeasternmost instrument (OBS 29) was located at a range of 319.84 km. After recalculation of the OBS locations, instrument positions were projected onto this baseline.

[17] The velocity model for the crust and uppermost mantle was developed using the programs RAYINVR and TRAMP [*Zelt and Smith*, 1992; *Zelt and Forsyth*, 1994]. First, observed travel times were fitted by forward model-
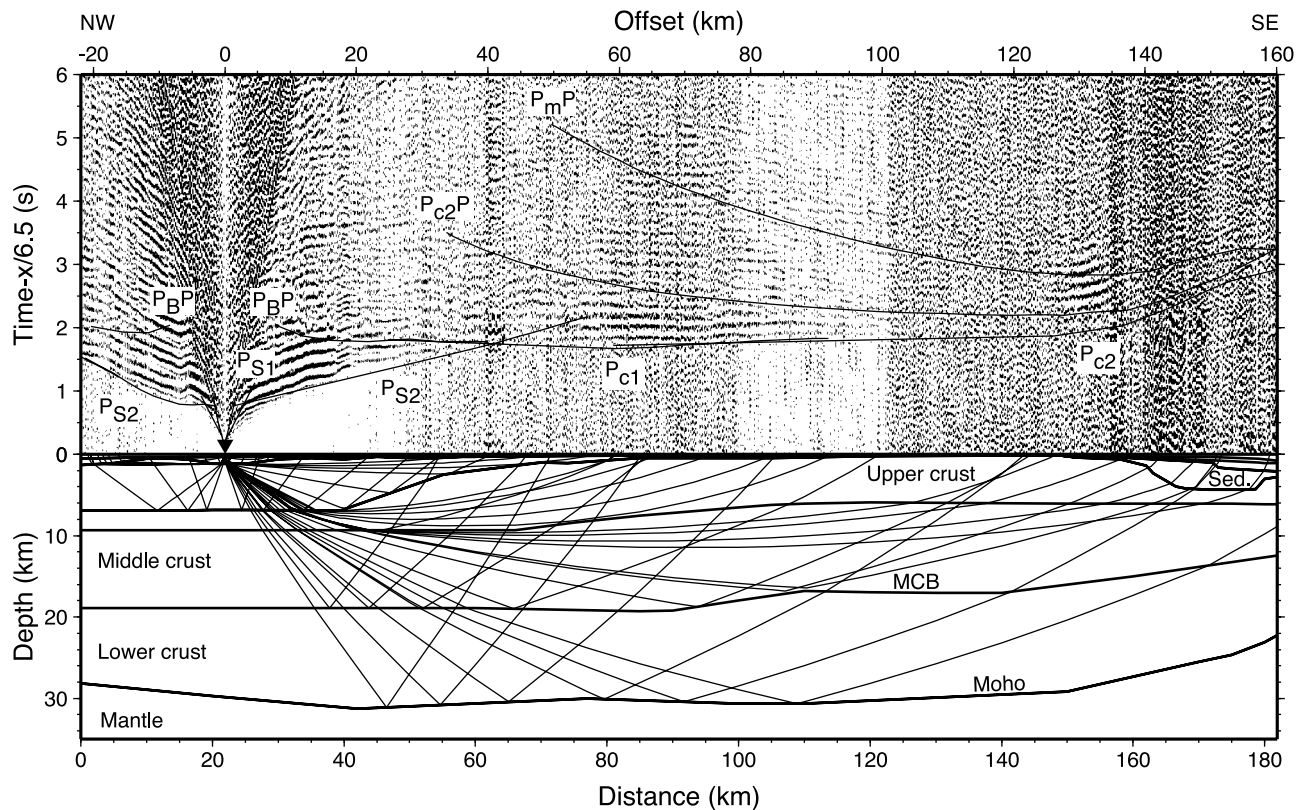
Figure 3. (top) Record section with computed travel times and (bottom) ray path diagram for the vertical geophone of OBS 2. Horizontal scale in the record section is shot-receiver distance (offset), and the vertical scale is the travel time using a reduction velocity of 6.5 km/s. A triangle indicates the receiver location. See text for description of phases and processing. The horizontal scale of the ray path diagram is distance along the velocity model (Figure 10). Abbreviations are MCB, midcrustal boundary; Sed., sediments.

ing, with the model being developed from top to bottom. Additional constraints were obtained from the coincident reflection seismic record [*Hopper et al.*, 2003] from km 202 to the seaward end of the line. These data define the sedimentary structure and the basement morphology in more detail than modeling of the wide-angle seismic data permits. After an initial model was obtained, velocities and the geometry of layer boundaries were refined using the inversion algorithm in RAYINVR. Amplitude information was considered in the modeling process by qualitative comparison of ray theoretical synthetic seismograms with the field records. The source signal used for the synthetic seismograms was extracted from a shot with a high signal-to-noise ratio at an offset of 28 km.

3.4. Seismic Data

[18] The seismic data are generally of good quality. Record sections (Figures 3–7) are shown together with the calculated travel times through the final velocity model to allow for a comparison how well the model fits the data. Names of individual seismic phases are based on the later interpretation of the velocity model.

[19] Record sections from stations deployed on Flemish Cap (Figures 3 and 4) show two internal crustal reflectors ($P_{c1}P$ and $P_{c2}P$), subdividing the crust into three layers (upper, middle and lower crust). Refractions within these

layers are labeled P_{c1}, P_{c2}, and P_{c3}, respectively. Amplitudes of the $P_{c1}P$ and $P_{c2}P$ reflections are low and indicate a small impedance contrast. However, for OBS 2 (Figure 3) a strong postcritical $P_{c2}P$ reflection is observed between offsets of 125 and 135 km. These high amplitudes fit well with results from amplitude modeling. The Moho reflection (P_mP) from the base of the crust has a higher amplitude. Figure 4 shows a rather complicated signature of the P_mP phase to the southeast on the outer continental margin when compared to the smoother shape of the phase to the northwest, where the rays are reflected from a more or less flat crust-mantle boundary.

[20] Sediments are identified in three separate areas along the line. One is located in the northwestern part of Flemish Cap, one extends from the slope break landward on the southeast margin, and the last one is the deep Newfoundland Basin. A maximum of three layers is sufficient to describe the velocity structure of the sediments and the according refracted phases are named P_{S1}, P_{S2}, and P_{S3} from top to bottom. Reflections from the base of sediment layers 1 and 2 are called $P_{S1}P$, and $P_{S2}P$, respectively, unless they are identical with the basement reflection (P_BP).

[21] OBS 19 (Figure 5) marks the seaward transition to a different crustal domain. This is the most seaward instrument that records a refraction (P_{c1}) with a phase velocity of ~6 km/s, which is indicative of upper continental crust. To
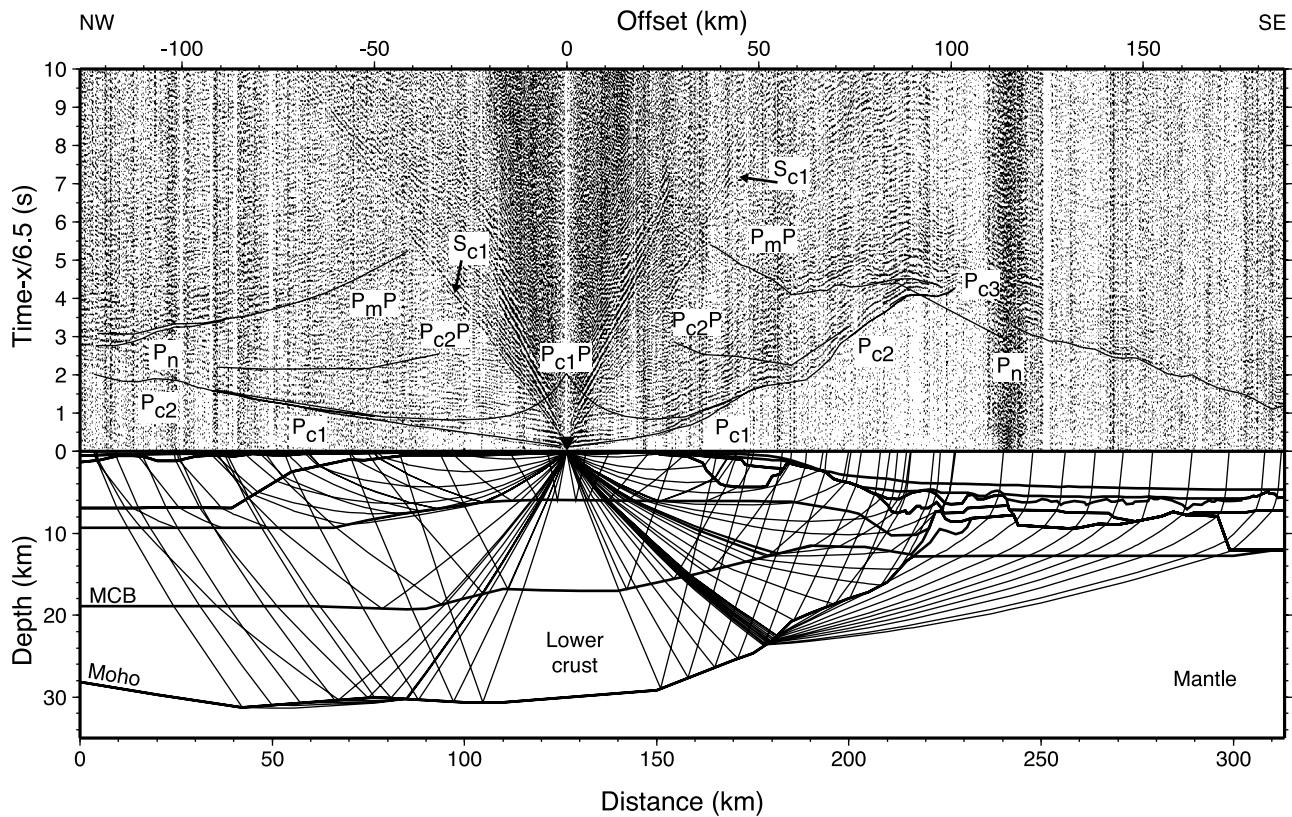
Figure 4. (top) Record section with computed travel times and (bottom) ray path diagram for the vertical geophone of OBS 7. Horizontal scale in the record section is shot-receiver distance (offset) and the vertical scale is the travel time using a reduction velocity of 6.5 km/s. A triangle indicates the receiver location. See text for description of phases and processing. The horizontal scale of the ray path diagram is distance along the velocity model (Figure 10). MCB is midcrustal boundary.

the southeast, two new seismic phases appear. The slower phase has a velocity slightly lower than 5.0 km/s, whereas the faster one is modeled with a velocity close to 7.0 km/s. These two refractions are named P_{L2} and P_{L3}, respectively. Phase P_{L3} is not observed on OBS 23 (Figure 6). Instead the lower-velocity layer appears to sit directly on top of mantle, creating a strong P_mP reflection at an offset of ~10 km with a triplication (P_{L2}, P_mP, and P_n, where P_n is the refraction within the upper mantle). P_n phases in Newfoundland Basin have high amplitudes over large ranges (Figure 7) indicating a higher velocity gradient than expected for normal mantle. Phase velocities are also <8.0 km/s. OBS 25 (Figure 7), for example has a P_n phase velocity of 7.7 km/s to the northwest. In summary, the uppermost mantle velocity structure beneath Newfoundland Basin appears to be different from "normal" mantle that is characterized by velocities around 8.0 km/s and a low-velocity gradient.

[22] Several stations show some surprisingly high-amplitude arrivals interpreted as diffractions based on their steep dips (e.g., Figures 5 and 6). These diffractions cannot be modeled with the ray-tracing program used in this study.

4. Results

4.1. Velocity Model

[23] The fit of the calculated to the observed travel times is illustrated in Figures 8 and 9. The corresponding P wave velocity model is shown in Figure 10. The central part of Flemish Cap from km 80 to km 150 is characterized by 30-km-thick crust that is subdivided into three layers. Velocities in the 7-km-thick upper crust vary between 6.0 and 6.2 km/s. The base of the upper crust is mapped almost continuously by weak wide-angle reflections ($P_{c1}P$). Midcrustal velocities range from 6.3 to 6.4 km/s with the midcrustal boundary located at a depth between 17 and 19 km. Lower crustal velocities are 6.6 to 6.7 km/s. Clear shear wave observations along the line are limited to the OBS with prominent upper crustal refractions S_{c1} in the central part of Flemish Cap (Figure 4). Computation of the phase velocities and comparison with the velocities of the corresponding P_{c1} phases yields P to S wave velocity ratios between 1.71 and 1.73 (Poisson's ratio between 0.24 and 0.25).

[24] No major sediment cover was detected on the central part of Flemish Cap. To the northwest, sediments with a velocity of 2.8 km/s and a maximum thickness of 900 m were found. They are deposited on top of a layer up to 6 km thick with a velocity of 5.4 km/s. The shape of this layer resembles a sedimentary basin although the velocities could well be within the range of igneous crust. The possible origin of this unit will be discussed later.

[25] Southeast of km 150, the continental crust of Flemish Cap thins abruptly. Close to the slope break there is a ~25-km-wide basin with up to 4 km of sediment. This
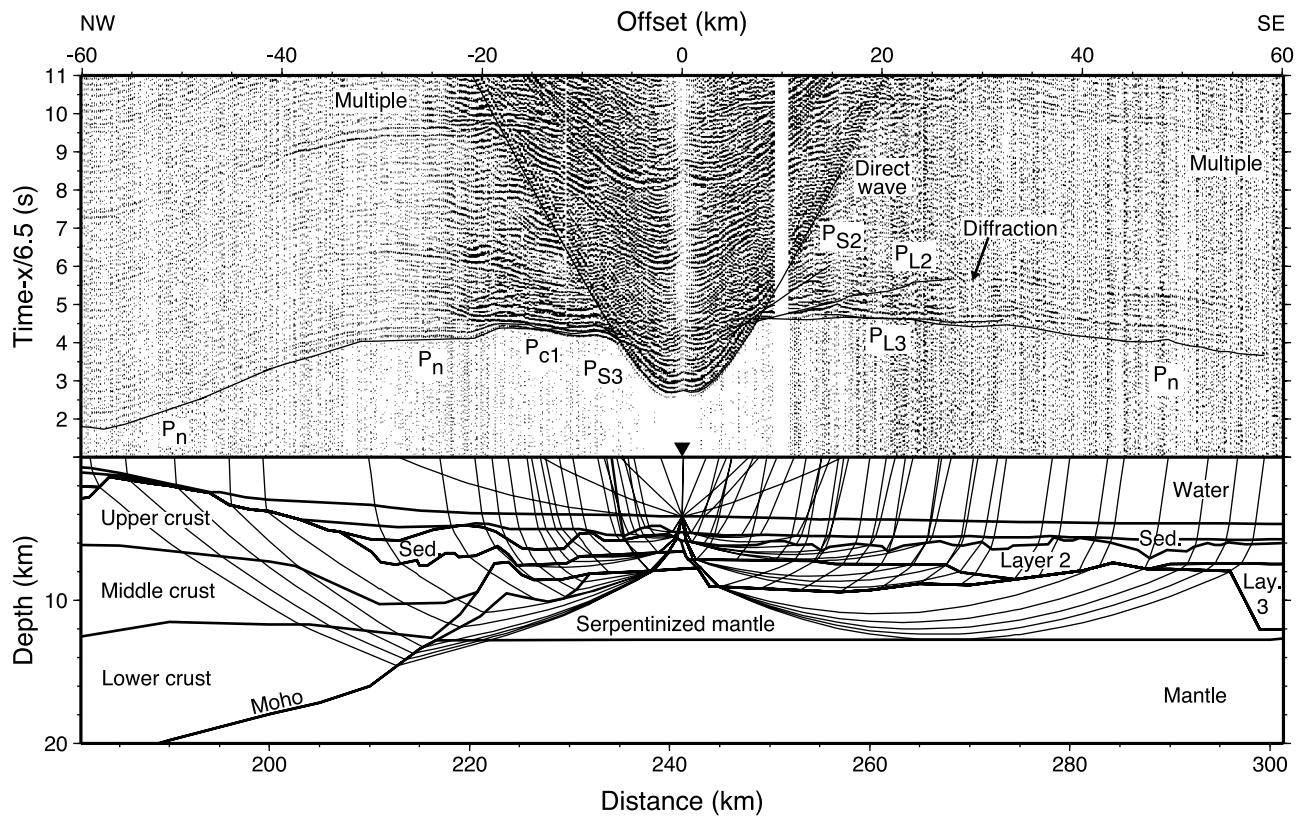
Figure 5. (top) Record section with computed travel times and (bottom) ray path diagram for the vertical geophone of OBS 19. Horizontal scale in the record section is shot-receiver distance (offset) and the vertical scale is the travel time using a reduction velocity of 6.5 km/s. A triangle indicates the receiver location. See text for description of phases and processing. The horizontal scale of the ray path diagram is distance along the velocity model (Figure 10). Abbreviations are Sed., sediments; Lay., layer.

basin is subdivided into three individual layers with velocities of 2.1, 3.1, and 4.6 km/s from top to bottom. At km 215, the crust is only 6 km thick and the middle crust has disappeared. Velocities similar to middle or lower crust (6.6 km/s) are found in a small sliver that extends from km 215 to km 231 with a thickness of up to 2 km. Farther seaward, a 1.5-km-thick layer with velocities similar to upper crust (6.1 km/s) extends up to km 242. The thin crust between km 210 and km 240 is covered with three sediment layers. The upper two layers are stratified units with velocities between 2.0 and 3.8 km/s, the lower layer consists of two distinctive features with a dome-like shape and a more chaotic reflection pattern [*Hopper et al.*, 2003]. Their velocities are 3.9 to 5.2 km/s in the northwest and 4.9 to 5.2 km/s in the southeast.

[26] Seaward of km 242 is a significant change of crustal velocity structure. Here the crust consists of two layers, an upper layer with a thickness between 1 and 2 km and velocities of 4.7 to 4.9 km/s, and a lower layer with a maximum thickness of 2 km and velocities of 6.8 to 7.0 km/s. No reflections are observed between these two layers, indicating a smooth velocity transition at the boundary. The lower layer disappears between km 274 and km 288. Farther seaward, the lower layer thickens again up to ~4 km, while velocities in the upper layer are reduced to 4.3–4.5 km/s. Here the crust resembles normal thickness oceanic crust with oceanic layers 2 and 3.

[27] Sediments in the deep Newfoundland Basin are seismically divided into two units, both of them with stratified layering [*Hopper et al.*, 2003]. The upper sedimentary unit has velocities of 1.9 to 2.2 km/s and a thickness of 1.2 km. The lower unit, where it is not missing in the areas of basement highs, has velocities around 3.0 km/s and is generally less than 1 km thick.

[28] Normal mantle velocities along the line are 8.0 km/s. However, beneath the thin crust (<6 km thickness) from km 217 to km 299, uppermost mantle velocities are significantly reduced. They are as low as 7.6 km/s directly beneath the thin crust and increase downward to a normal mantle velocity of 8.0 km/s at a depth of ~6 km below the top of the basement. This zone of reduced velocities is interpreted as serpentinized mantle.

4.2. Model Resolution and Uncertainty

[29] Travel time residuals, number of observations, and normalized χ^2 for individual phases are summarized in Table 1. The total misfit is 105 ms. The estimated pick uncertainty varied between 30 ms for high-amplitude observations close to the OBS and 250 ms for weak P_n arrivals. Using these uncertainties, the normalized χ^2 for the experiment is 1.394, which is close to the optimum value of 1. It should be noted that the spacing of the travel time picks was set to 500 m, to be able to separate individual picks during the modeling process and to avoid bias toward stations
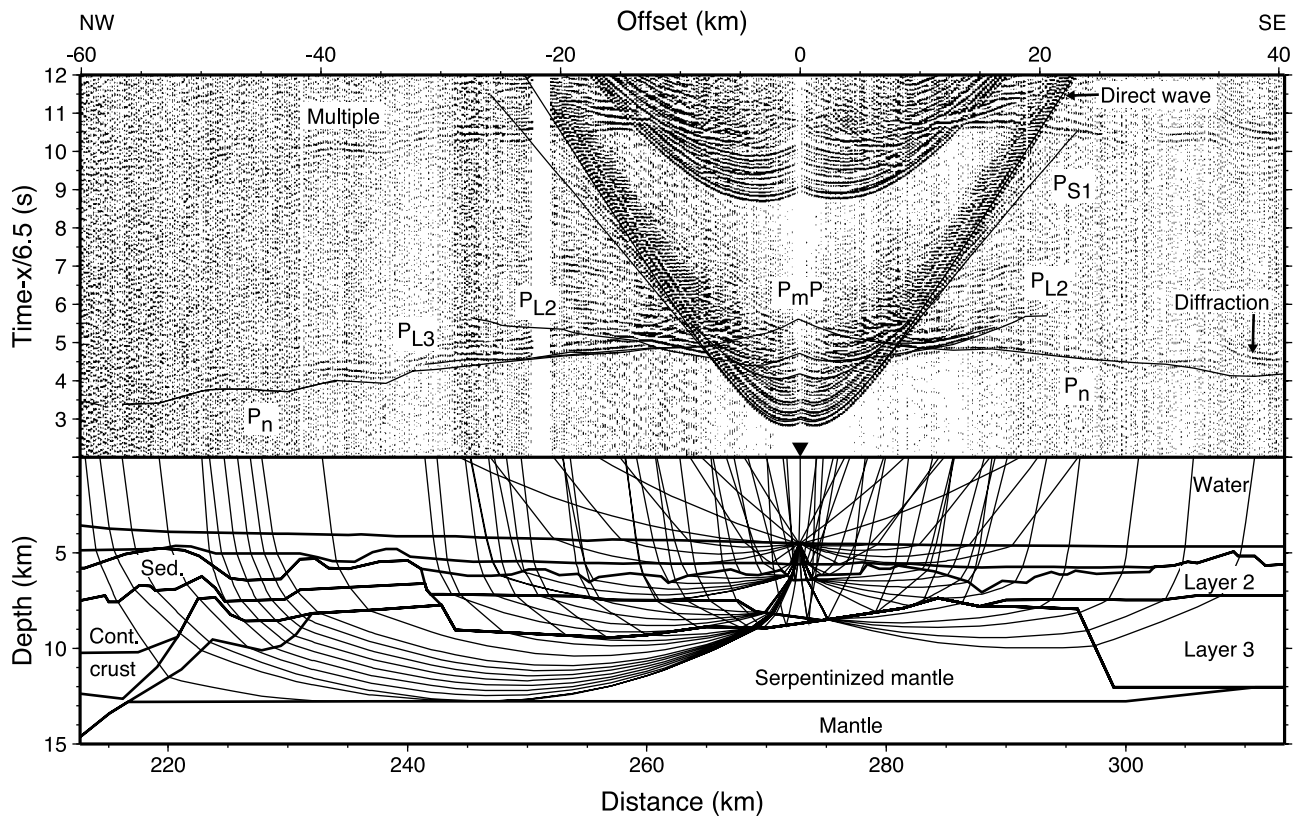
Figure 6. (top) Record section with computed travel times and (bottom) ray path diagram for the hydrophone of OBS 23. Horizontal scale in the record section is shot-receiver distance (offset) and the vertical scale is the travel time using a reduction velocity of 6.5 km/s. A triangle indicates the receiver location. See text for description of phases and processing. The horizontal scale of the ray path diagram is distance along the velocity model (Figure 10). Abbreviations are Sed., sediments; Cont., continental.

where travel times were picked from the coincident MCS line with a shot spacing of only 50 m.

[30] Figure 10 shows the values of the diagonal of the resolution matrix for the velocity nodes of the model. Ideally, these values are 1, with values less than 1 indicating spatial averaging of the true Earth's structure by a linear combination of model parameters [*Zelt*, 1999]. Resolution matrix diagonals of greater than $0.5-0.7$ indicate reasonably well resolved model parameters [*Lutter and Nowack*, 1990]. Resolution is excellent within the thick continental crust of Flemish Cap with diagonal values of 0.9 in the central part. Toward the northwest the resolution decreases as the model boundary is approached and the ray coverage is less dense. The velocity model is characterized by a number of layer pinch-outs. Velocity nodes at the pinch-out locations are singularities where the resolution is zero. This explains a generally low crustal resolution between km 200 and km 250.

[31] The small crustal block around km 225 with a velocity of 6.6 km/s is poorly resolved (resolution <0.1). However, it is well imaged in the reflection seismic record [*Hopper et al.*, 2003] where good picks from the reflection travel time modeling of focusing analysis indicate a velocity of ~6.6 km/s. Changing this velocity by more than 0.3 km/s results in a blurred image of the reflectors. Moreover, the boundaries of the block are characterized by strong reflectivity, which requires some impedance contrast to the neighboring structure. This accords with the velocity model (Figure 10) where the crust adjacent to the block has velocities between 6.0 and 6.4 km/s and the underlying mantle is modeled with 7.6 to 8.0 km/s.

[32] Resolution within the sediments is often reduced (Figure 10), particularly in the basin northwest of the slope break. Some of this can be attributed to the effects of layer pinch-outs, but the main cause is a lack of overlapping ray coverage. The lowermost sediment layer in Newfoundland Basin between km 200 and km 240 has a resolution of <0.2, which according to *Lutter and Nowack* [1990] has to be considered as not constrained. However, the 42 observations of P_{S3} phases within that layer have a travel time residual of 102 ms (Table 1), which is similar to the overall error. Again, velocities and geometry obtained from the coincident MCS line [*Hopper et al.*, 2003] guided the modeling here and is in accord with the few observations in the R/WAR seismic data. A similar argument can be used for the upper crustal layer (layer 2) southwest of km 242 where the resolution is <0.5 except for two small isolated areas around km 270 and km 295. Refractions (P_{L2}) within this layer are often not reversed, and generally, the phase cannot be correlated very far from the OBS. This results formally in a low resolution. However, the basement, which is guiding the refraction, is well known from the reflection seismic record [*Hopper et al.*, 2003], and it eliminates the ambiguity resulting from nonreversed observations.

[33] Velocity resolution within the mantle is good with values around 0.8 (Figure 10). Lower resolution at the
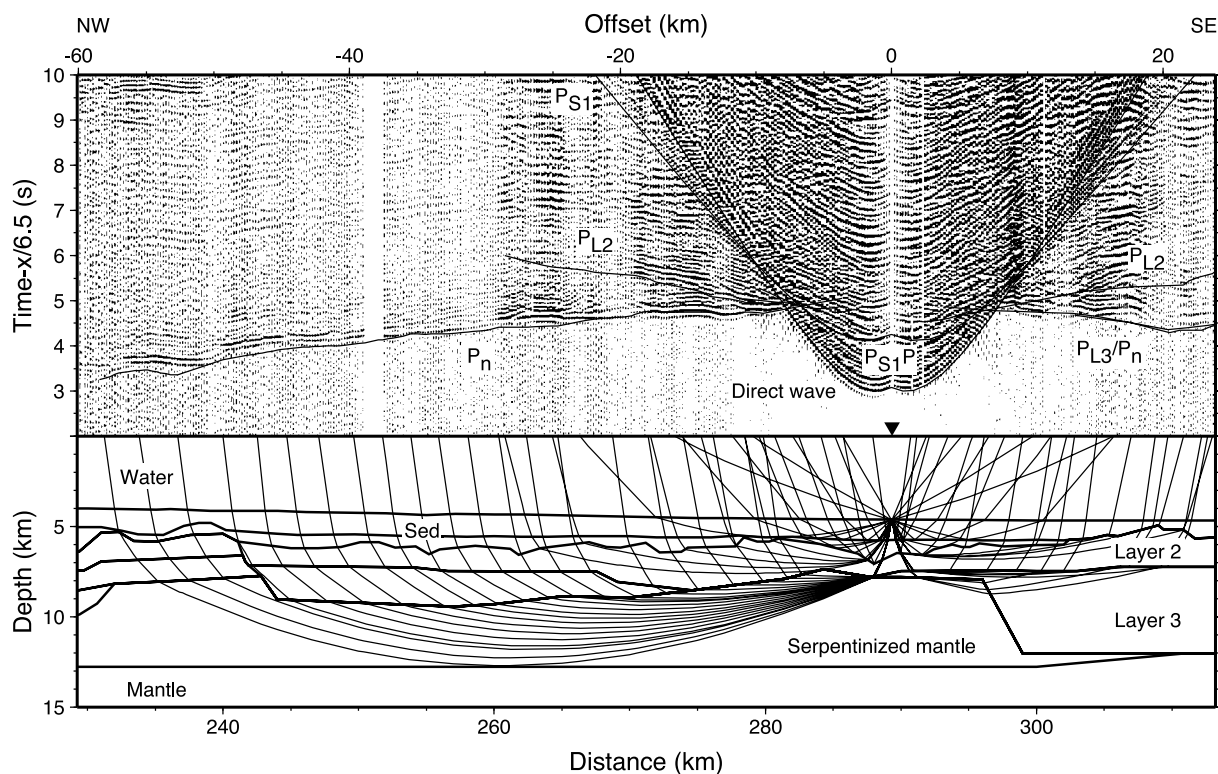
Figure 7. (top) Record section with computed travel times and (bottom) ray path diagram for the vertical geophone of OBS 25. Horizontal scale in the record section is shot-receiver distance (offset) and the vertical scale is the travel time using a reduction velocity of 6.5 km/s. A triangle indicates the receiver location. See text for description of phases and processing. The horizontal scale of the ray path diagram is distance along the velocity model (Figure 10). Abbreviation is Sed., sediments.

northwestern and southeastern limit of the serpentinized mantle can be related to layer pinch-out and proximity to the model boundary.

[34] The only area that is of some concern with respect to resolution is located southeast of OBS 26 (297 km). Here the shooting ship had to make way for fishing long lines and was forced 6.5 km to the north of the baseline on which the OBS were deployed. The MCS record along the baseline [*Hopper et al.*, 2003] shows two basement highs in this segment, around km 309 and km 318, respectively (see also Figure 10). Much of the data misfit is obviously related to the possibility that these highs are local features and not ridges that extend off the line. In addition, instrument relocations of OBS 27 and 28 have higher uncertainties due to the larger distances to the shots. It is difficult to quantify the possible error in velocity in the southeast. The largest impact should be on the upper crustal layer because it is affected most by the basement morphology. Some of the reduced velocities in the upper crustal layer (4.3– 4.5 km/s), compared to 4.7–4.9 km/s farther to the NW, are likely related to these geometry problems.

[35] The steep southeastern flank of the serpentinized mantle around km 298 (Figure 10) is mostly required by OBS 28, where the P_n phase would otherwise arrive too early. Other OBS are less sensitive and can be modeled with the flank dipping less steeply. Irrespective of the dip, crustal thickening is required at the southeastern end of the line.

[36] Most layer boundaries are well defined by either wide-angle reflections (Figure 10), in the cases of subbasement structures, or by the coincident MCS record [*Hopper et al.*, 2003] in the cases of sedimentary layers and basement. The least constrained is the transition from serpentinized mantle to normal mantle. In the velocity model (Figure 10), the 8.0 km/s contour, which marks the boundary between serpentinized mantle with a high-velocity gradient and the normal mantle with a low gradient, is put at a depth of 12.75 km. At this depth, the travel time residual of the P_n phase is a minimum (124 ms). Variations of 1 km in the depth result in an increase of 6 ms in the residual, which is not a very significant variation. Stronger evidence in support of this depth is the amplitude variation. Once the P_n rays bottom in the low-gradient normal mantle, their amplitudes decrease. The P_n phase for OBS 26 (Figure 11) is relatively strong up to km 234 (corresponding to an offset of −63 km) and then it becomes so weak that travel time picking becomes difficult. With the base of the serpentinized mantle at 12.75 km/s, strong P_n arrivals can be expected up to km 238, which is a good match with the observation. Changing the depth to 11.75 km or 13.75 km would move the distance to km 251 and km 225, respectively. This is a variation that is well resolvable and it provides confidence that the depth error of the boundary (second-order velocity discontinuity) is well within 1 km.

4.3. Gravity Modeling

[37] Two-dimensional gravity modeling (algorithm of *Talwani et al.* [1959]) was performed along the line to verify how consistent the velocity model is with the gravity

Figure 8. Comparison of observed and calculated travel times for OBS 2–16, shown together with the corresponding ray paths. Observed data are indicated by vertical bars, with heights representing pick uncertainty; calculated data are indicated by solid lines. Triangles mark the receiver locations. Horizontal scale is the model position; a reduction velocity of 6.5 km/s has been applied for the travel times. Abbreviation Dir. is the direct wave.
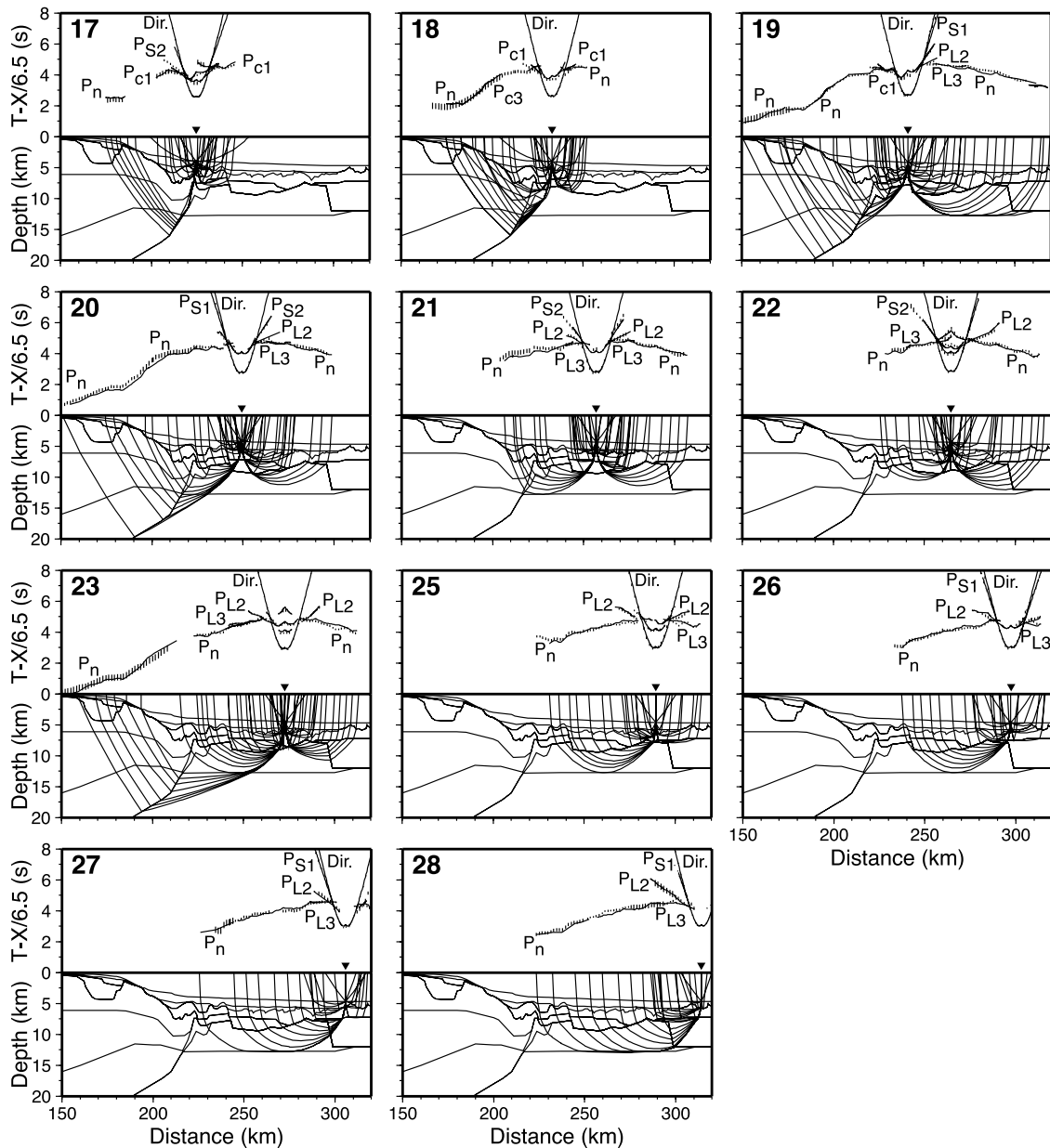
Figure 9. Same as Figure 8 for OBS 17–28.

data. Free-air gravity anomalies were obtained from the shipboard gravimeter on R/V *Maurice Ewing* (Figure 12). The initial density model was derived from conversion of P wave velocities to density using the empirical formula of *Ludwig et al.* [1970]

$$\rho = -0.00283v^4 + 0.0704v^3 - 0.598v^2 + 2.23v - 0.7$$

with ρ the density in g/cm^3 and v the P wave velocity in km/s. When the gravity model was extended to infinity to avoid edge effects, there was a significant misfit in the northwest due to the proximity of the end of the line to the rift basin in Flemish Pass. This lateral change in crustal structure immediately northwest of line 1 is illustrated by the decrease of the free-air gravity anomaly from Flemish Cap to Flemish Pass (Figure 13b). In the absence of

detailed velocity information in Flemish Pass from other data, we raised the Moho depth to 23 km in the northwest extension of the model to take some of the basin structure into account. This value is close to the 22 km reported by *Keen and Barrett* [1981].

[38] Another necessary change at the northwestern end of the line was an increase in density from 2.58 to 2.66 g/cm^3 in the 5.4 km/s near-surface layer. Even with this adjustment there remains a considerable misfit of up to 21 mGal between the observed and calculated gravity in this area. The 5.4 km/s layer may not be a truly two-dimensional feature. At least to the west the layer is intercepted by the Flemish Cap Basin (Figures 2 and 13b).

[39] To fit the long-wavelength pattern of the gravity signal, lateral density changes within the mantle had to be introduced. With the base of the model at a depth of 65 km,
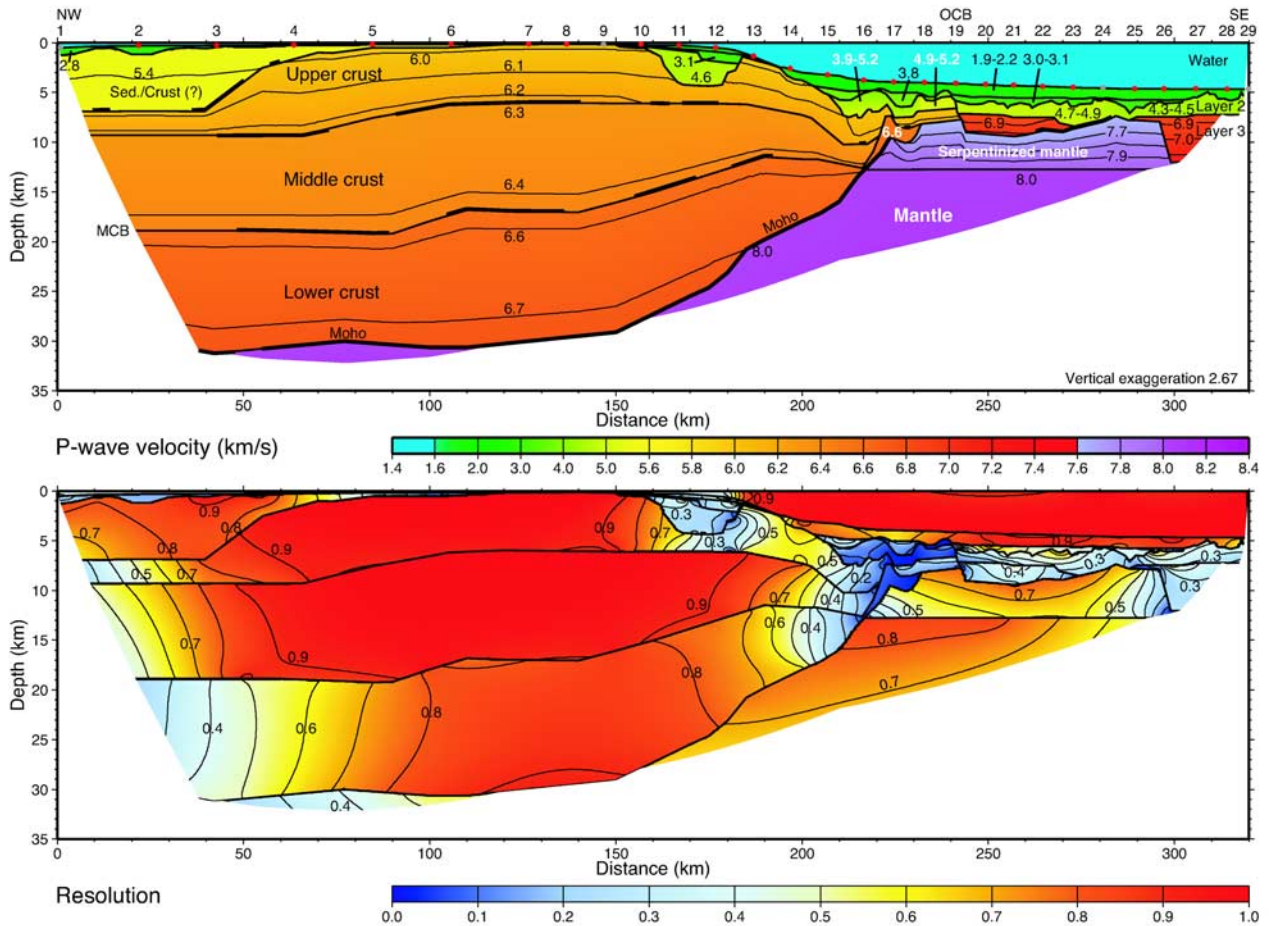
Figure 10. (top) *P* wave velocity model with a contour interval (thin solid lines) of 0.1 km/s between 5.4 and 8.0 km/s. Numbers indicate velocity, in km/s. White numbers indicate areas that are primarily constrained by focusing analysis of the coincident reflection seismic data [*Hopper et al.*, 2003]. The outer perimeter of the model with no ray coverage is omitted. Layer boundaries constrained by reflections are drawn with bold solid lines. Red circles mark the location of OBS used for the modeling, gray circles show the location of OBS with no data recovery. Station numbers are indicated at the top of the image. (bottom) Diagonal values of the resolution matrix of the *P* wave velocity model displayed in contour format (0.1 contour interval). Abbreviations are Sed., sediments; MCB, midcrustal boundary; OCB, ocean-continent boundary.

mantle densities beneath the thinned continental crust and farther seaward were set to 3.27–3.29 g/cm^3. Beneath the full thickness continental crust of Flemish Cap, a density of 3.32–3.33 g/cm^3 was used. Finally, the density within the serpentinized mantle from km 231 to km 244 was reduced from 3.24 to 3.20 g/cm^3 compared to our initial model, while densities in the lower crustal layer (layer 3) seaward of km 242 were increased by 0.10 g/cm^3.

[40] The adjusted density model (Figure 12) fits the slope anomaly very well, both in terms of the amplitude and shape of the anomaly. Some misfits can probably be attributed to deviations from the two dimensionality of the model, as inferred for the northwestern end of the line. Another such zone is the sedimentary basin between km 160 and km 185, which is associated with a local reduction in the calculated gravity by about 10 mGal. An equivalent signal is missing in observed gravity, which may be an indication of limited extent of the basin perpendicular to the line. The density model is approximately isostatically balanced at its base

(65 km), where the lithostatic pressure is 1950 MPa with variations of <20 MPa (Figure 12).

5. Discussion

5.1. Continental Crust

[41] The velocity model obtained for the central part of Flemish Cap is consistent with other observations within the Avalon Zone of the Appalachians, to which *King et al.* [1985] correlates Flemish Cap. On a line 10 km east of Newfoundland (line 91-2, Figure 2), *Marillier et al.* [1994] report velocities between 5.7 and 6.3 km/s in the upper Avalon crust and 6.8 km/s at its base near 35 km depth. Within other zones of the Newfoundland Appalachians, velocities at the top of the crust are also close to 6.0 km/s and those at the base normally do not exceed 7.0 km/s (see summary of *Hall et al.* [1998]). In the Appalachians north of Newfoundland, *Funck et al.* [2001] found a velocity structure almost identical to line 1 across Flemish Cap. They

Table 1. Number of Observations (n), RMS Misfit Between Calculated and Picked Travel Times (t_{rms}), and Normalized χ^2 for Individual Phases

| Phase	n	t_{rms}, s	χ^2
Direct wave	854	0.075	1.858
P_{S1} (Basin NW Flemish Cap)	20	0.078	0.708
P_{S2} (Basin NW Flemish Cap)	196	0.065	1.376
P_BP (Basin NW Flemish Cap)	44	0.063	0.637
P_{S1} (Basin slope break)	8	0.041	0.298
P_{S2} (Basin slope break)	16	0.039	0.177
P_{S3} (Basin slope break)	51	0.066	1.760
P_{S1} (Newfoundland Basin)	89	0.108	2.181
$P_{S1}P$ (Newfoundland Basin)	124	0.101	1.918
P_{S2} (Newfoundland Basin)	80	0.149	4.128
$P_{S2}P$ (Newfoundland Basin)	34	0.138	3.158
P_{S3} (Newfoundland Basin)	42	0.102	3.432
P_BP (Newfoundland Basin)	100	0.107	2.479
P_{c1}	1623	0.065	1.015
$P_{c1}P$	257	0.088	1.053
P_{c2}	1174	0.132	1.630
$P_{c2}P$	588	0.105	0.642
P_{c3}	40	0.129	1.993
P_{L2}	212	0.087	1.281
P_{L3}	220	0.094	2.643
P_mP	1652	0.113	1.014
P_n	1780	0.124	1.487
All phases	9204	0.105	1.394

also report a reflective boundary between the upper and middle crust at a depth of ~10 km, similar to line 1. Upper crustal *P* wave velocities of ~6.0 km/s and a Poisson's ratio of 0.24–0.25 are indicative of granite, granodiorite or gneiss [*Holbrook et al.*, 1992]. These results are consistent with rock samples from Flemish Cap, which indicate granodiorite as the major component and minor granite [*King et al.*, 1985].

[42] The 6-km-thick layer with a velocity of 5.4 km/s at the northwestern end of line 1 is difficult to interpret. The velocity could indicate either high-velocity sedimentary rocks or rather low-velocity igneous crust. The shape of the unit has similarity to a sedimentary basin, but there is no recognizable stratification on the coincident reflection seismic record or along MCS line 85-3 which crosses it (Figure 2) [*Keen et al.*, 1987]. The highest sedimentary or possibly basement velocity in the adjacent Flemish Pass basin is 4.8 km/s [*Keen and Barrett*, 1981], and there is no equivalent to the 5.4 km/s layer within Flemish Pass or farther seaward along line 1. Hence it seems unlikely that the 5.4 km/s layer is a sediment or sediment/basalt fill associated with Late Triassic rifting along the Newfoundland margin. Either the layer consists of older (meta)sediments or it is indeed basement. Basement velocities of 5.4 km/s are absent elsewhere in the Newfoundland Appalachians, which suggests that the unit may be prerift sediments or mixed sedimentary/igneous rocks. Age and thickness of the unit must have resulted in compaction or low-grade metamorphism, which could contribute to the lack of reflectivity within the unit. Refraction seismic line 91-2 (Figure 2) parallel to the coast off Newfoundland shows velocities increasing from 4.6 km/s through 5.2 to 5.7 km/s over the top 5 km [*Marillier et al.*, 1994; *Hall et al.*, 1998] and probably correspond to the Precambrian sediments and volcanics of the Avalon terrane. Similar "basement" velocities (5.0–5.3 km/s) are observed in the Galicia Interior Basin on the conjugate Iberia margin

[*Pérez-Gussinyé et al.*, 2003], but the composition of these rocks is unknown.

[43] The weak wide-angle reflections observed at mid-crustal levels at Flemish Cap appear to be related to prerift structures within the continental crust. Reflection seismic line 85-3 across Flemish Cap (Figure 2) shows midcrustal reflectivity that can be correlated over wide zones [*Keen et al.*, 1987]. On the southeast side of Flemish Cap, thinning of the continental crust starts at km 140 and includes all crustal layers. The midcrustal layer disappears first at km 220, while a thin sliver with velocities of 6.6 km/s continues as far as km 232. From there, only thin upper crust extends seaward for another 10 km, with crustal thickness around
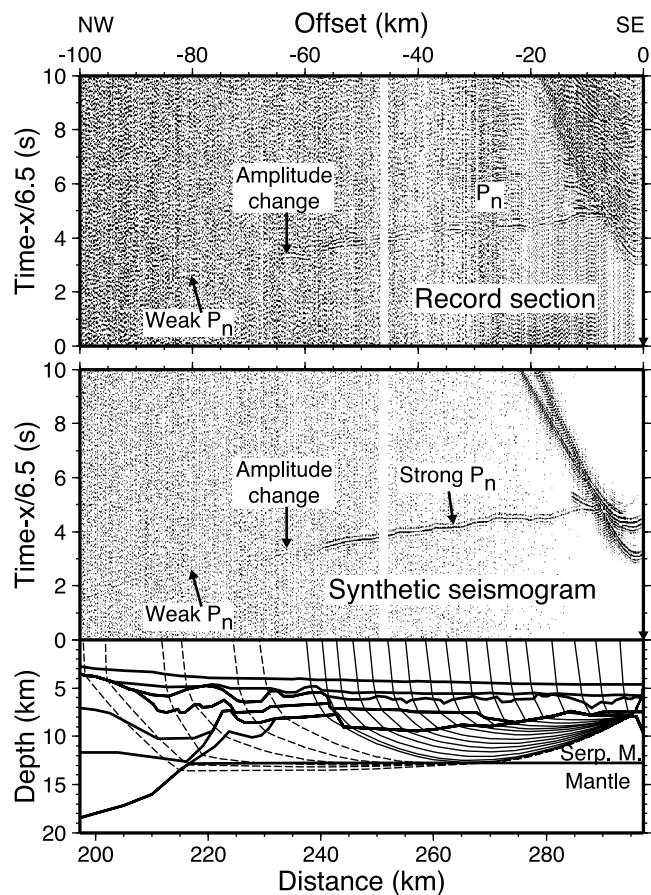
Figure 11. (top) Record section of OBS 26 (middle) compared to the corresponding synthetic seismogram. Horizontal scale in the record section is shot-receiver distance (offset) and the vertical scale is the travel time using a reduction velocity of 6.5 km/s. A triangle indicates the receiver location. Processing of the record section includes a 6-Hz notch filter on some traces, deconvolution, band-pass filter (4.5–11 Hz), and trace scaling by range. The synthetic seismogram is band-pass filtered and scaled in the same way with some Gaussian noise added. (bottom) The horizontal scale of the ray path diagram is distance along the velocity model (Figure 10). Rays with bottom points in the partially serpentinized mantle are drawn as solid lines, and rays that reach into the normal mantle are shown as dashed lines. Abbreviation Serp. M., serpentinized mantle.
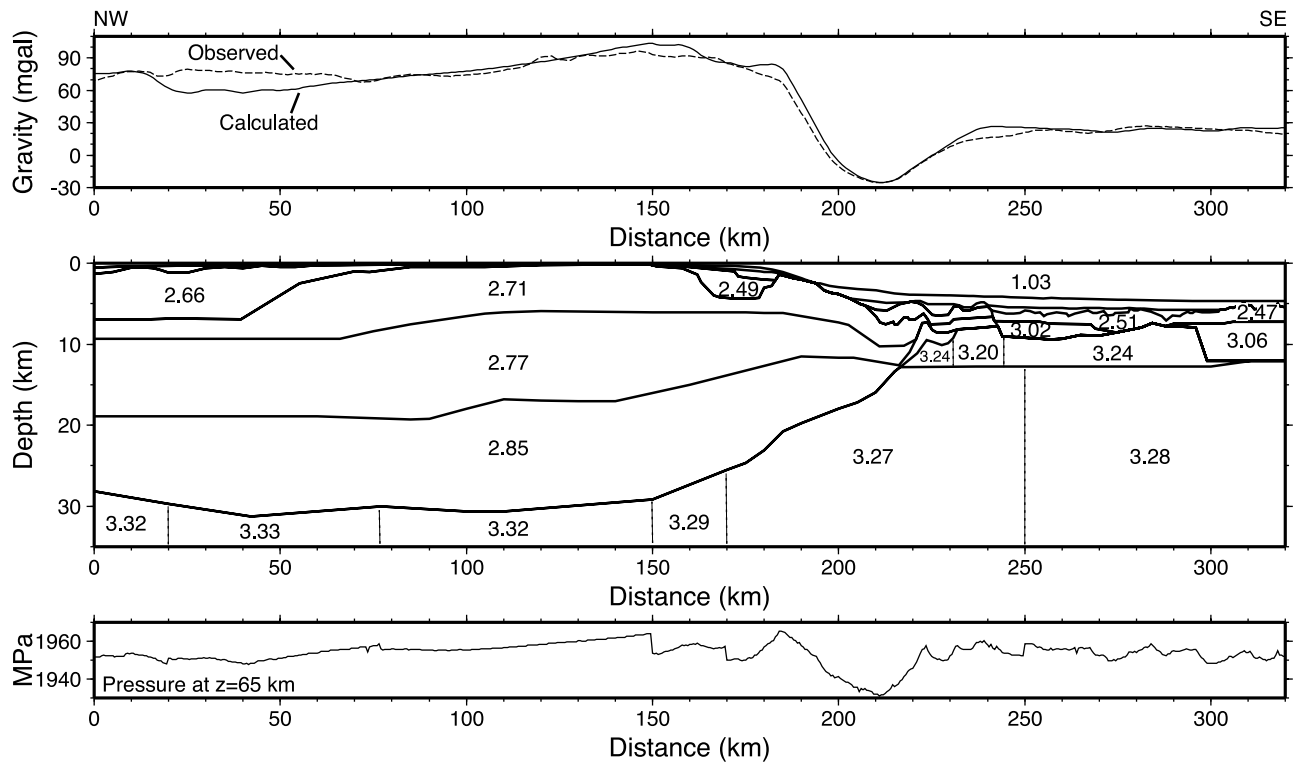
Figure 12. Two-dimensional gravity modeling for line 1. The *P* wave velocity model (Figure 10) was converted to density using the velocity-density relationship of *Ludwig et al.* [1970] with additional modification as discussed in the text. Densities in the model (middle) are given in g/cm^3. (top) Observed and calculated gravity anomalies are shown by dashed and solid lines, respectively. (bottom) The lithostatic pressure at the base of the model (depth of 65 km) is shown as solid line.

1.2 km, compared to 30.4 km maximum crustal thickness at Flemish Cap. This yields a crustal thinning factor β of 25. However, even with these extreme amounts of crustal extension there is no indication of major magmatic activity.

5.2. Ocean-Continent Transition

[44] Between the thinned continental crust and what appears to be close to normal thickness oceanic crust is a 55-km-wide zone of transitional crust with a thickness between 2 and 3 km (Figure 10). The boundary between the continental and transitional crust is located just seaward of a sediment-capped block at km 240 with velocities around 5.0 km/s. This feature is interpreted as continental crust of unknown origin based on the velocities and the reflection pattern [*Hopper et al.*, 2003]. The coincident reflection seismic line shows a faulted contact between the two crustal types around km 242 [*Hopper et al.*, 2003].

[45] To evaluate the character of the transitional crust, three possible models are considered here: (1) thinned continental crust, (2) exhumed and serpentinized upper mantle, and (3) igneous crust generated by a slow spreading ridge. There are clear arguments against continental crust. Velocities in the transitional crust (4.8 km/s in the upper crust and 6.9 km/s below) are not compatible with velocities found in the continental crust at Flemish Cap (6.0 to 6.7 km/s). The 4.8 km/s layer might be attributed to crustal modifications by faulting, brecciation and hydrothermal alterations; however, the deeper 6.9 km/s layer has significantly higher velocity than any lower continental

crust to the west, and it is distinctly different from the very thin continental crust immediately to the west. Only if this crust was heavily intruded by igneous mafic material would it be likely to have these high velocities.

[46] The second alternative is that the transitional crust is exhumed and highly serpentinized upper mantle continuous with the underlying layer with velocities of 7.6 to 8.0 km/s representing less deeply serpentinized mantle. Hence velocities in the transitional crust would range from 4.7 to 8.0 km/s and would be comparable to values obtained from the conjugate Galicia Bank (3.5–7.8 km/s) [*Whitmarsh et al.*, 1996] where the velocity gradient has been related to decreasing serpentinization with depth. The largest problem in explaining the transitional crust in this manner is that velocity is layered within three distinct units. In addition, large sections of the top of the lowermost serpentinized unit (7.6–8.0 km/s) are characterized by wide-angle reflections, and an even wider zone exhibits high-amplitude normal incidence reflectivity suggesting a concordantly stratified upper crust [*Hopper et al.*, 2003]. Such prominent and laterally continuous reflections within the serpentinized mantle are not known from other studies and are much more likely to represent volcanic strata.

[47] In the transition zone of the southern Iberia Abyssal Plain (IAP), the velocity model of *Dean et al.* [2000] shows two layers (velocities between 4.3 and 7.3 km/s) overlying serpentinized mantle with velocities between 7.3 and 7.9 km/s. The preferred model for the two upper layers is that they consist of mantle peridotite serpentinized between
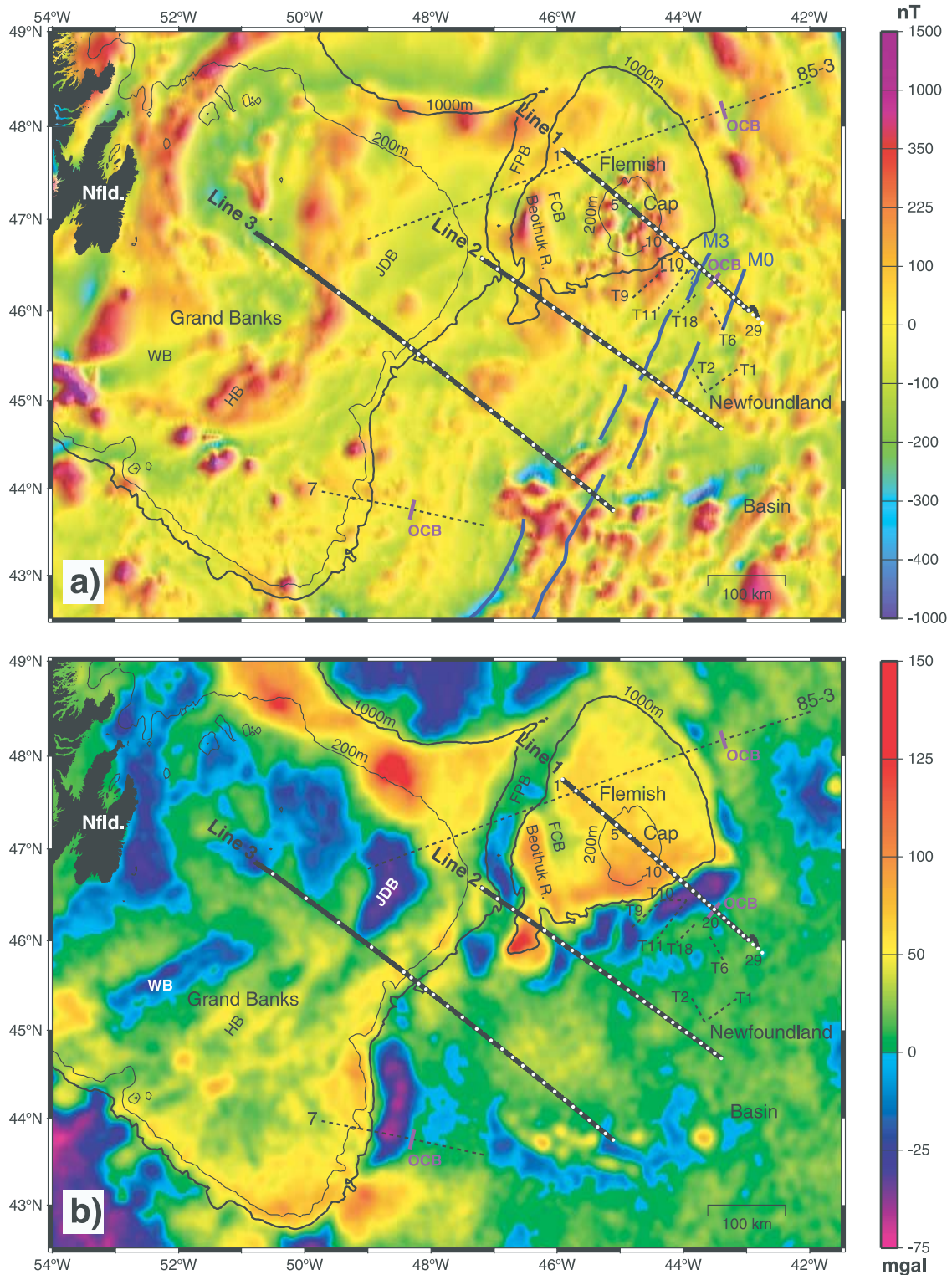
Figure 13. (a) Magnetic anomaly map and (b) free-air gravity anomaly map. Magnetic data are taken from *Verhoef et al.* [1996], and gravity data are taken from *Sandwell and Smith* [1997]. Bold solid lines show the shot lines of the SCREECH experiment with circles indicating the location of OBS. Reflection seismic line 85-3 [*Keen et al.*, 1987] and refraction lines 7 [*Reid*, 1994] and T1-T18 [*Todd and Reid*, 1989] are drawn with dashed lines. Blue lines indicate the location of magnetic anomalies M0 and M3 [*Srivastava et al.*, 2000]. The 200- and 1000-m-depth contours of the bathymetry are drawn as solid lines. The shading of the magnetic anomalies is by illumination from the east. Abbreviations are Nfld., Newfoundland; OCB, interpreted ocean-continent boundary; FCB, Flemish Cap Basin; FPB, Flemish Pass Basin; JDB, Jeanne d'Arc Basin; WB, Whale Basin; HB, Horseshoe Basin; R., Ridge.

25 and 100%. While the velocities are not too dissimilar to those found in the transition zone of line 1 (4.7 to 7.0 km/s), there are some differences that may indicate another composition. The combined thickness of the two upper layers in the southern IAP stays fairly constant at about 3 km, which indicates that the amount of serpentinization as a function of depth is more or less similar throughout the transition zone. However, on line 1 in Newfoundland Basin, basement above the 7.6 km/s serpentinite layer has a more variable thickness between 1 and 3.5 km. At the location of the thinnest crust (~km 290, Figure 10), the crust appears to be more intensely faulted than in other areas [*Hopper et al.*, 2003]. Because faulting normally facilitates serpentinization by providing pathways for water, we would expect a higher degree of serpentinization and, hence, low *P* wave velocities reaching greater depths at this location. However, the opposite is observed. Another difference between the two transition zones is the reflection character above the ~7.6 km/s serpentinite layer. In the southern IAP, there is an upper unreflective layer on top of a reflective layer [*Pickup et al.*, 1996; *Dean et al.*, 2000], while the MCS record on line 1 [*Hopper et al.*, 2003] shows high reflectivity at the top and reduced reflectivity below. *Pickup et al.* [1996] do not see reflectivity in the upper 1–1.5 s, while all the reflectivity on our line 1 is in the upper second [*Hopper et al.*, 2003].

[48] The third alternative to explain the transition zone is that it is magma-starved oceanic crust accreted during slow or ultraslow spreading. Velocities within the two layers of the transitional crust between km 240 and 270 fit those of oceanic layers 2 and 3. In oceanic crust, layer 2 has an average thickness of 2.11 ± 0.55 km and velocities between 2.5 and 6.6 km/s, while layer 3 has velocities of 6.69 ± 0.26 km/s [*White et al.*, 1992]. Variations in oceanic crustal thickness are mainly related to thickness variations within layer 3, while the thickness of layer 2 remains fairly constant [*Mutter and Mutter*, 1993]. A refraction seismic study of the ultraslow spreading Mohns Ridge (16 mm/yr full spreading rate) reveals a total crustal thickness of 4 km with a close-to-normal thickness layer 2 (1.4–1.7 km), while oceanic layer 3 appears to be thinned compared to normal oceanic crust [*Klingelhöfer et al.*, 2000]. The transitional crust on line 1 can be interpreted in these terms. Layer 2 is observed everywhere with a thickness of 1 to 2 km, while thinning of the crust coincides with thinning or even complete absence of layer 3. Thin oceanic crust (2 to 4 km) underlain by serpentinized mantle is reported off western Iberia [*Pinheiro et al.*, 1992; *Whitmarsh et al.*, 1993, 1996]. Presently, the slowest spreading ridge in the world is the Gakkel Ridge (<10 mm/yr full spreading rate); based on gravity studies there, *Coakley and Cochran* [1998] estimate the crustal thickness at 1 to 4 km, which fits with our observations on line 1. Results from a refraction seismic experiment across the Gakkel Ridge show the presence of thin (1.9 to 3.3 km) oceanic crust with absence of layer 3 on most records [*Jokat et al.*, 2003]. Velocities in the uppermost mantle are between 7.5 and 7.8 km/s and are attributed to partly serpentinized mantle. This structure is very similar to our transitional crust at Flemish Cap.

[49] In summary, the velocity structure in the transition zone is compatible with thin oceanic crust created by ultraslow seafloor spreading with limited and/or episodic magma supply operating in parallel with tectonic extension. Extensional faults and fractures within the crust provided pathways for seawater to reach and partially serpentinize the underlying uppermost mantle. On the basis of this interpretation, the ocean-continent boundary (OCB) is located at km 242, at the location of OBS 19 (Figure 10). This location is marked on the potential field maps in Figure 13. On the free-air gravity map (Figure 13b), the OCB is located just seaward of the prominent gravity low (−30 mGal) along the continental rise and slope. Farther seaward, the gravity signature is rather smooth with values of ~30 mGal (see also Figure 12). The OCB on line 1 appears to be abrupt rather than transitional as at the Iberia/Galicia margin where there is a zone of exhumed continental mantle between the continental crust and igneous oceanic crust [*Whitmarsh et al.*, 1996; *Dean et al.*, 2000].

[50] On the magnetic anomaly map, the OCB plots at a position where the pattern changes from a long-wavelength magnetic low (−200 nT) in the northwest to a more irregular pattern with shorter wavelengths and anomalies in the order of ±100 nT to the southeast. The irregular pattern continues seaward of line 1, and *Srivastava et al.* [2000] interpret this region to be created by slow seafloor spreading based on magnetic evidence. In the area crossed by line 1, they identified magnetic anomalies M0 and M3. Anomaly M0 lies seaward of our interpreted OCB, but M3 is located well within the zone that is clearly thinned continental crust. Hence M0 appears to be the oldest magnetic anomaly along the northernmost segment of the Newfoundland margin that can be explained by seafloor spreading.

[51] The OCB position is consistent with interpreted OCBs elsewhere along the margin. A refraction seismic line (line 7, Figure 2) on southern Grand Banks [*Reid*, 1994] shows thin, probably basaltic crust (1 to 4 km thick with velocities of ~4.5 km/s) on the eastern segment of the line, underlain by serpentinized mantle. The interpreted OCB is located just seaward of the prominent slope anomaly in gravity (Figure 13b), similar to line 1. Northeast of Flemish Cap, the conjugate to Goban Spur (Figure 1), *Keen et al.* [1987] locate the OCB on reflection seismic line 85-3 in a position also similar to that on line 1 (Figure 13). The slope anomaly in gravity is less pronounced on line 85-3, but oceanic crust is interpreted to start ~15 km seaward of the trough. The magnetic pattern along the oceanic part of line 85-3 also resembles that on line 1.

[52] *Todd and Reid* [1989] obtained seven short refraction lines just south of line 1 (Figure 13), and they interpret the OCB in a position very similar to line 1. Their lines T9-T11 lie within the gravity slope anomaly (Figure 13b) and show velocities typical of continental crust. Farther seaward (line T18), a 1.5-km-thick layer with velocities of 4.5 km/s is observed, which *Todd and Reid* [1989] interpret as oceanic crust. The underlying layer with velocities of 7.3 km/s was originally thought to be oceanic layer 3. However, *Reid* [1994] reinterpreted this layer to be possible serpentinized mantle, which fits well with our interpretation of line 1.

[53] The crust at the seaward end of line 1 is interpreted to be oceanic crust of close to normal thickness despite the reduced resolution seaward of km 300 as pointed out in the error analysis. The available data indicate a division of the crust in two layers with velocities in the order of 4.5 and

7 km/s, respectively, and crustal thickening is required by several OBS. These velocities, even with higher uncertainties, would be difficult to explain with continental crust or serpentinized mantle. Magnetic interpretations of *Srivastava et al.* [2000] support an oceanic character as well.

5.3. Mantle Serpentinization

[54] The velocity model (Figure 10) shows a layer with velocities of 7.6−8.0 km/s in an 80-km-wide zone underlying the thinned continental crust and the thin transitional crust with oceanic character. This layer is interpreted as partially serpentinized mantle and it is analogous to similar layers at other nonvolcanic rifted margins, for example off Iberia [*Whitmarsh et al.*, 1996; *Chian et al.*, 1999; *Dean et al.*, 2000], Greenland and Labrador [*Chian and Louden*, 1994; *Chian et al.*, 1995a, 1995b], and the southern Grand Banks [*Reid*, 1994]. The velocity range observed on line 1 suggests a serpentinite fraction of <10% in the mantle [*Miller and Christensen*, 1997].

[55] *Pérez-Gussinyé and Reston* [2001] correlate the onset of serpentinization beneath continental crust with embrittlement of the entire crust during progressive extension. Once all of the overlying crust is in the brittle regime, seawater can reach the mantle through connected networks of faults and fractures to initiate serpentinization of the mantle. The entire crust becomes brittle at a stretching factor β_b between ∼3 and 5, depending on the strain rate [*Pérez-Gussinyé and Reston*, 2001]. On line 1, apparently serpentinized mantle first appears beneath crust ∼8 to 4 km thick. With an original crustal thickness of 30.4 km, this corresponds to β_b = 3.8 to 7.6. These values compare well with a factor of 5.3 obtained for the Iberia Abyssal Plain [*Pérez-Gussinyé et al.*, 2001].

[56] The high-velocity layer (7.6−8.0 km/s) beneath the thin oceanic crust is interpreted in a similar way. The thin oceanic crust is characterized by numerous faults, many of which can be traced down to the Moho [*Hopper et al.*, 2003], and it is likely seawater penetrated to, and serpentinized, the upper mantle. Velocities of 7.6 km/s within the serpentinized mantle are similar to 7.5 km/s mantle velocities found beneath thin oceanic crust at the ultraslow spreading Mohns Ridge [*Klingelhöfer et al.*, 2000] or the Gakkel Ridge [*Jokat et al.*, 2003].

5.4. Comparison With Conjugate Margin

[57] Line 1 at Flemish Cap is conjugate to R/WAR seismic line 6 [*Whitmarsh et al.*, 1996] at the western margin of Galicia Bank. Velocity models show strong similarities between the lines. At Galicia Bank, a 60-km-wide zone with serpentinized mantle underlies both thin continental crust and, farther seaward, thin oceanic crust (Figure 14). A peridotite ridge separates oceanic from continental crust. At Galicia Bank, the serpentinized mantle has velocities between 7.2 and 7.6 km/s in the deeper parts and as low as 3.5 km/s in the peridotite ridge exposed at the seafloor. Velocities at the top of oceanic layer 2 vary between 4.6 and 4.8 km/s. Within layer 3, velocities are near 7.0 km/s. All these velocities are similar to our line 1.

[58] The thickness of the oceanic crust overlying the serpentinized mantle varies between 2.5 and 3.5 km, which is very similar to the Flemish Cap margin. *Whitmarsh et al.* [1996] attribute the limited melt generation and thus the thin oceanic crust to cooling of slowly upwelling mantle by conductive heat loss during a long period of stretching of the continental lithosphere prior to breakup. In addition, the spreading rate probably was low; *Srivastava et al.* [2000] assumed a full rate of ∼14 mm/yr.

[59] There are some limitations when comparing the continental sections on either side of the rift. On the Galicia side, the existing profiles continue onto relatively unextended continental crust. At Flemish Cap, the extension of SCREECH line 1 would run into Flemish Pass and farther into Orphan Basin (Figure 1). However, the continental crust in Orphan Basin [*Chian et al.*, 2001] was extended during a later phase of rifting at ∼110 Ma [*Srivastava et al.*, 1988]. This prevents a full reconstruction of the prerift structure of our line 1. Nevertheless, with these limitations in mind, we see some differences between the two margins (Figure 14). Most notably, the crustal thinning at Galicia extends over a wider zone. Beneath Galicia Bank maximum crustal thickness is on the order of 20−22 km [*Whitmarsh et al.*, 1996; *González et al.*, 1999] and in Galicia Interior Basin, between Galicia Bank and Iberia, crust thins to as little as 12 km [*González et al.*, 1999]. Full thickness continental crust in northwest Iberia is ∼32 km [*Cordoba et al.*, 1987]. This value is comparable to the maximum Moho depth of ∼30 km at Flemish Cap. All the continental crust seaward of the Iberia mainland has been extended. Initial rifting occurred in Triassic-Liassic time, but it appears to have concentrated in Galicia Interior Basin in the Early Cretaceous (Valanginian) and then on the seaward margin of Galicia Bank beginning in Hauterivian time, prior to breakup [*Murillas et al.*, 1990]. Similar rift phases [*Tankard and Welsink*, 1987; *Driscoll et al.*, 1995] formed basins in the Grand Banks, including Flemish Pass Basin, but they appear not to have extended the crust of Flemish Cap.

[60] According to *Whitmarsh et al.* [1996], the continental crust at Galicia Bank is divided into only two layers with velocities between 5.2 and 6.9 km/s, whereas the Flemish Cap crust exhibits three layers with velocities ranging from 6.0 to 6.7 km/s. From these results, it would appear that the two continental blocks have different internal structure or composition. However, *González et al.* [1999] modeled the Galicia crust with three layers of velocity 6.0−6.1 km/s, 6.4−6.5 km/s, and 6.8−6.9 km/s, similar to our results at Flemish Cap (Figure 10). The *Whitmarsh et al.* [1996] results were constrained with just two OBS deployments along the continental segment, so uncertainties in these data may explain some of the differences with our Flemish Cap results.

[61] Figure 14a shows a reconstruction of the Flemish Cap-Galicia Bank rift at the time of initial seafloor spreading, i.e., matching the contact between the continental and oceanic crust at Flemish Cap with the western limit of the peridotite ridge off Galicia [*Whitmarsh et al.*, 1996]. The reconstruction shows that the final breakup position, with respect to distribution of thinned continental crust, is skewed to the Canadian side of the rift. The Flemish Cap margin appears very narrow and abrupt whereas the conjugate is a broad zone of thinned continental crust. This is similar to models of rifting that examine possible causes of asymmetric margin pairs that show wide rift mode of extension is likely to preferentially break along one edge, leaving a narrow/wide conjugate margin pair [*Dunbar and Sawyer*, 1989; *Hopper and Buck*, 1996]. As would be
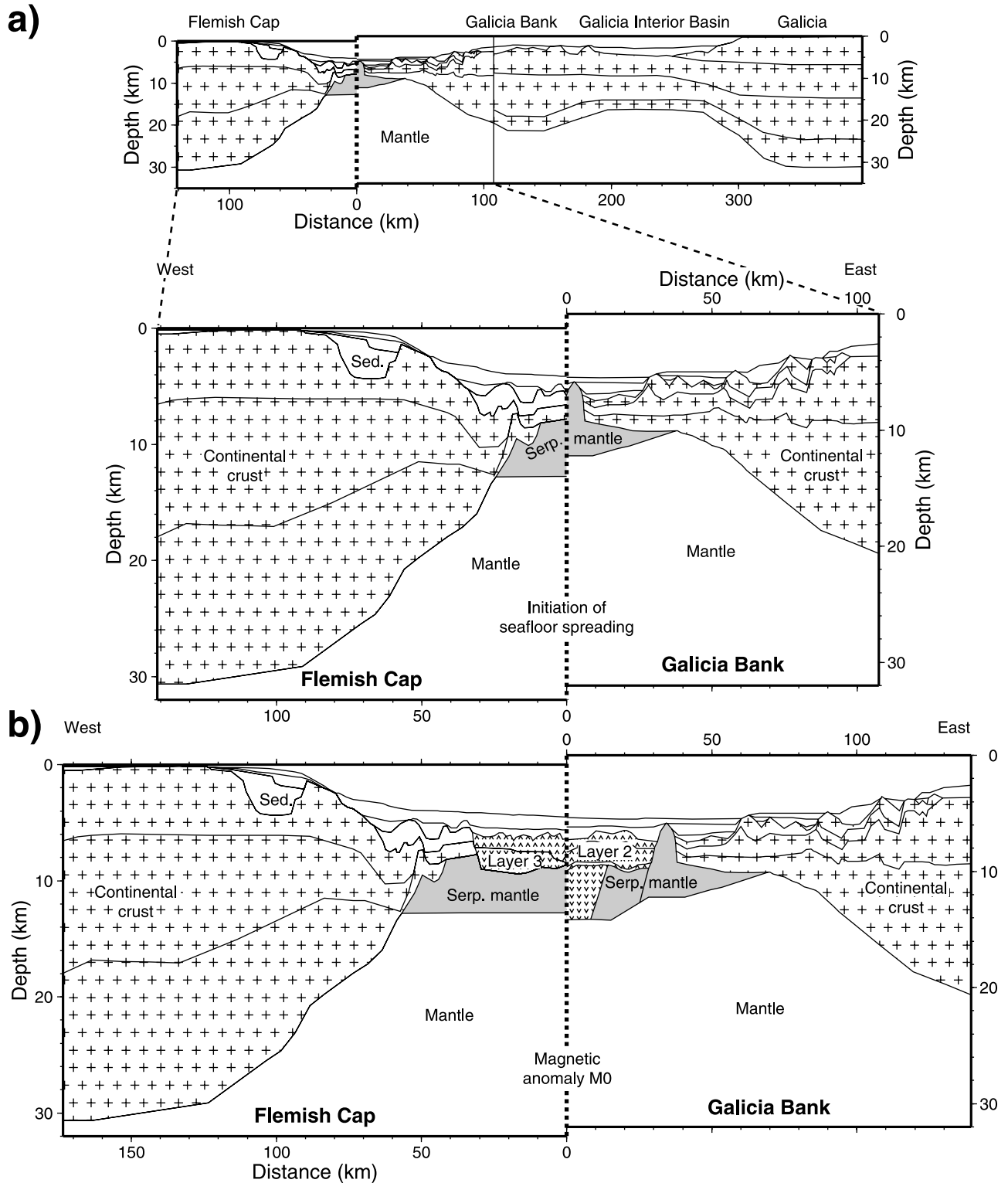
Figure 14. Reconstruction of the cross sections of the Flemish Cap-Galicia Bank margins at (a) the initiation of seafloor spreading and (b) at the time of magnetic anomaly M0 (118 Ma) using the identification of magnetic anomalies given by *Srivastava et al.* [2000]. The model for Galicia Bank is taken from *Whitmarsh et al.* [1996]; the model for the Galicia Interior Basin and Galicia is from *González et al.* [1999]. Horizontal scale is distance from the ridge/spreading axis (dashed line). Continental crust is marked by pluses, oceanic layer 3 is marked by v's, layer 2 is marked by inverted v's, and serpentinized mantle by gray shading. Abbreviations are Sed., sediments; Serp., serpentinized.

expected from the distribution of thinned continental crust, Galicia Bank experienced more intense faulting than Flemish Cap [*Reston et al.*, 1996; *Mauffret and Montadert*, 1987]. Prominent and extensive detachment faults known as "S" reflections developed under continental extension on the Galicia margin [*Reston et al.*, 1996]. At Flemish Cap, there is no evidence for subhorizontal detachments in continental crust [*Hopper et al.*, 2003]. A final asymmetry is observed in basement depth. Galicia crust is on the order of 1 km deeper than Flemish Cap crust at the OCB (Figure 14a) and this asymmetry persists into the oldest ocean crust (Figure 14b).

[62] Figure 14b reconstructs the Flemish Cap to the Galicia Bank margin at the time of magnetic anomaly M0 (118 Ma) as identified by *Srivastava et al.* [2000]. The reconstruction indicates a 32-km-wide zone of oceanic crust on the Flemish Cap side, very similar to the 31 km found at Galicia, and it suggests a symmetric seafloor spreading pattern following final breakup. Using a half-spreading rate of ∼7 mm/yr as assumed by *Srivastava et al.* [2000], the onset of seafloor spreading dates to ∼4.5 m.y. prior to magnetic anomaly M0 (∼123 Ma, Barremian on the timescale of *Kent and Gradstein* [1986]).

[63] While seafloor spreading appears to be symmetric between the conjugate margins (Figure 14b), there are differences in thickness of oceanic crust on the two sides. At Galicia Bank, the zone with 2.5- to 3.5-km-thin oceanic crust is only 17 km wide before the crust thickens seaward to ∼7 km. In contrast, all the oceanic crust landward of anomaly M0 at Flemish Cap is only 3 km thick. The resulting 4 km misfit at M0 could relate either to problems with identification of magnetic anomalies or to problems with the velocity models. Some caution certainly is required when using the magnetic interpretations of *Srivastava et al.* [2000]. For instance, their location of magnetic anomaly M3 at Flemish Cap (Figure 13a) lies within crust that appears to be continental according to our velocity model and MCS interpretations. If both the Flemish Cap and Galicia velocity models are correct, then a rather awkward model of asymmetric melt accretion or a ridge jump is required to explain the differences in crustal thickness. In the latter case, very asymmetric seafloor spreading must have occurred prior to anomaly M0.

[64] Alternatively, it is possible that the velocity models are incorrect. The thickness of the oceanic crust at Flemish Cap is well constrained northwest of OBS 26 (Figure 10). We therefore revisit the experiment of *Whitmarsh et al.* [1996] to examine whether their model would permit any modifications. It is noteworthy that the two conjugate lines would fit very well if the interpreted lower oceanic crust (layer 3) at Galicia Bank was actually serpentinized mantle (Figure 14b). First, looking at the gravity model presented by *Whitmarsh et al.* [1996, Figure 9], one can see that the observed gravity (−18 mGal) shows no deviation at the transition between the thin oceanic crust and normal-thickness oceanic crust. However, the calculated gravity shows a seaward drop of ∼12 mGal at the transition. A better fit between observed and calculated gravity could be obtained by continuing the serpentinized mantle farther seaward.

[65] If we examine the Galicia seismic data, it is important to note that only three OBS were deployed along line 6, and the segment of oceanic crust in question was not constrained primarily by observations from line 6 but from a cross line. This cross line likewise had only three OBS deployments and the crossing point was close to the southern end of the line where resolution was generally reduced. On the cross line, velocities in layer 3 were modeled with 7.1–7.2 km/s, which is rather high for layer 3, and velocities in the underlying mantle were modeled with 7.6 km/s, which is rather low for mantle. The southernmost OBS showed almost no lateral amplitude variation in first arrivals, while the synthetic seismogram computed from the velocity model exhibited striking variations, sometimes with almost no energy at all. The amplitudes for this station could be fitted much better if layer 3 had a higher velocity gradient and a smooth transition into mantle velocities at the bottom. This model would merge the separate refraction branches (7.2 and 7.6 km/s) into one branch without large lateral amplitude variations, and it would be compatible with the conjugate Flemish Cap line, i.e., thin oceanic crust underlain by partially serpentinized mantle. Hence a reanalysis of this section of the Galicia velocity model is justified before we attempt firm conclusions about the symmetry or asymmetry of pre-M0 oceanic crust.

6. Conclusions

[66] Our refraction seismic study across the southeastern Flemish Cap continental margin shows a 30-km-thick section of continental crust with velocities distributed in three layers: 6.0–6.2 km/s, 6.3–6.4 km/s, and 6.6–6.7 km/s. These velocities are similar to those of Appalachian crust known from other studies. The continental crust thins dramatically to only 1.2 km over a distance of ∼90 km, where a fault marks the contact with thin oceanic crust farther seaward. The first ∼55 km of oceanic crust that accreted to the margin has a thickness of ∼3 km but it thins locally to only ∼1 km. It is divided into two layers: layer 2 with velocities of 4.7 to 4.9 km/s and layer 3 with a velocity of 6.9 km/s. Observed variations in oceanic crustal thickness correlate closely with thickness variations in layer 3, and there is a complete absence of layer 3 when total crustal thickness decreases to less than ∼1.5 km. We attribute the occurrence of this unusually thin oceanic crust to ultraslow seafloor spreading. Assuming a full-spreading rate of ∼14 mm/y [*Srivastava et al.*, 2000], the ∼55-km-wide zone of thin ocean crust represents about 8 m.y. of seafloor spreading, beginning near 123 Ma (Barremian). At the seaward end of our profile, the observed seismic phases are modeled with a velocity structure similar to normal thickness oceanic crust, although the resolution in this zone is reduced.

[67] Both the zone of thin oceanic crust (55 km wide) and the zone of continental crust stretched to a thickness of less than 6 km (22 km wide) are underlain by partially serpentinized mantle with velocities between 7.6 and 8.0 km/s. Theoretical calculations of *Pérez-Gussinyé and Reston* [2001] indicate that the entire continental crust becomes brittle when stretched by more than a factor, β_b, and this can provide pathways for seawater to reach the mantle and initiate serpentinization. At Flemish Cap, the factor β_b is ∼4–8. This is consistent with estimates of $\beta_b = 5.3$ by *Pérez-Gussinyé and Reston* [2001] for the Iberia

margin. We observe no tectonic exposure of upper mantle such as that in the peridotite ridge at the seaward margin of Galicia Bank or in an extensive, 130-km-wide zone beneath Iberia Abyssal Plain south of Galicia Bank [*Pickup et al.*, 1996].

[68] On the basis of magnetic anomalies identified by *Srivastava et al.* [2000], about 30 km of oceanic crust was accreted on both the Flemish Cap and Galicia margins between the onset of seafloor spreading and magnetic anomaly M0. Although the results of *Whitmarsh et al.* [1996] indicate that the outer part of this crust had normal thickness and velocity on the Galicia margin, an examination of their data suggests that this crust might actually be thin and overlie serpentinized mantle, much as we observe on the Flemish Cap margin. If this proves to be the case, the oceanic crust would be much more symmetric around the ridge axis at the time of anomaly M0. Neither side of the spreading axis shows evidence for significant synrift magmatism, as attested to by the unusually thin crust and an absence of any high-velocity underplated crustal layers.

[69] Extension of the continental crust in this rift occurred over a wide zone, bounded on both sides by sharp decreases from normal crustal thicknesses of ∼30 km to thicknesses of <2 km (Flemish margin) to ∼12 km (Iberia margin, descending into the Galicia Interior Basin). On the basis of presently observed crustal thicknesses, extension factors varied widely through the rift, ranging from $\beta \sim 1.5$ beneath Galicia Bank, to $\beta \sim 2.3$ in Galicia Interior Basin, to $\beta \sim 15{-}25$ at the juncture of Flemish Cap with the outer margin of Galicia Bank. These reflect a complex interplay of multiple zones of rifting over several rift episodes that began in late Triassic time and continued in to the Early Cretaceous. Final breakup about Barremian time focused extension near the foot of Flemish Cap, asymmetrically isolating most rifted continental crust on the Iberia margin.

References

Boillot, G., E. L. Winterer, A. W. Meyer, and Shipboard Scientific Party, *Proceedings of the Ocean Drilling Program, Initial Reports*, vol. 103, 663 pp., Ocean Drill. Program, College Station, Tex., 1987.

Chian, D., and K. E. Louden, The continent-ocean crustal transition across the southwest Greenland margin, *J. Geophys. Res.*, 99, 9117–9135, 1994.

Chian, D., C. Keen, I. Reid, and K. E. Louden, Evolution of nonvolcanic rifted margins: New results from the conjugate margins of the Labrador Sea, *Geology*, 23, 589–592, 1995a.

Chian, D., K. E. Louden, and I. Reid, Crustal structure of the Labrador Sea conjugate margin and implications for the formation of nonvolcanic continental margins, *J. Geophys. Res.*, 100, 24,239–24,253, 1995b.

Chian, D., K. E. Louden, T. A. Minshull, and R. B. Whitmarsh, Deep structure of the ocean-continent transition in the southern Iberia Abyssal Plain from seismic refraction profiles: Ocean Drilling Program (Legs 149 and 173) transect, *J. Geophys. Res.*, 104, 7443–7462, 1999.

Chian, D., I. D. Reid, and H. R. Jackson, Crustal structure beneath Orphan Basin and implications for nonvolcanic continental rifting, *J. Geophys. Res.*, 106, 10,923–10,940, 2001.

Coakley, B. J., and J. R. Cochran, Gravity evidence of very thin crust at the Gakkel Ridge (Arctic Ocean), *Earth Planet. Sci. Lett.*, 162, 81–95, 1998.

Cordoba, D., E. Banda, and J. Ansorge, The Hercynian crust in northwestern Spain: A seismic survey, *Tectonophysics*, 132, 321–333, 1987.

Dean, S. M., T. A. Minshull, R. B. Whitmarsh, and K. E. Louden, Deep structure of the ocean-continent transition in the southern Iberia Abyssal Plain from seismic refraction profiles: The IAM-9 transect at 40°20′N, *J. Geophys. Res.*, 105, 5859–5885, 2000.

Discovery 215 Working Group, Deep structure in the vicinity of the ocean-continent transition zone under the southern Iberia Abyssal Plain, *Geology*, 26, 743–746, 1998.

Driscoll, N. W., J. R. Hogg, N. Christie-Blick, and G. D. Karner, Extensional tectonics in the Jeanne d'Arc Basin, offshore Newfoundland: Implications for the timing of break-up between Grand Banks and Iberia, in *The Tectonics, Sedimentation and Palaeoceanography of the North Atlantic Region*, edited by R. A. Scrutton et al., *Geol. Soc. Spec. Publ.*, 90, 1–28, 1995.

Dunbar, J. A., and D. S. Sawyer, Patterns of continental extension along the conjugate margins of the Central and North Atlantic Oceans and Labrador Sea, *Tectonics*, 8, 1059–1077, 1989.

Funck, T., K. E. Louden, and I. D. Reid, Crustal structure of the Grenville Province in southeastern Labrador from refraction seismic data: Evidence for a high-velocity lower crustal wedge, *Can. J. Earth Sci.*, 38, 1463–1478, 2001.

González, A., D. Córdoba, and D. Vales, Seismic crustal structure of Galicia continental margin, NW Iberian Peninsula, *Geophys. Res. Lett.*, 26, 1061–1064, 1999.

Grant, A. C., and K. D. McAlpine, The continental margin around Newfoundland, in *Geology of Canada*, vol. 2, *Geology of the Continental Margin of Eastern Canada*, edited by M. J. Keen and G. J. Williams, pp. 239–292, Geol. Surv. of Can., Ottawa, 1990.

Hall, J., F. Marillier, and S. Dehler, Geophysical studies of the structure of the Appalachian orogen in the Atlantic borderlands of Canada, *Can. J. Earth Sci.*, 35, 1205–1221, 1998.

Holbrook, W. S., W. D. Mooney, and N. I. Christensen, The seismic velocity structure of the deep continental crust, in *Continental Lower Crust*, edited by D. M. Fountain, R. Arculus, and R. Kay, pp. 1–43, Elsevier Sci., New York, 1992.

Hopper, J. R., and W. R. Buck, The effect of lower crustal flow on continental extension and passive margin formation, *J. Geophys. Res.*, 101, 20,175–20,194, 1996.

Hopper, J. R., T. Funck, B. E. Tucholke, H. C. Larsen, W. S. Holbrook, K. E. Louden, D. Shillington, and H. Lau, Continental breakup and the onset of ultra-slow seafloor spreading off Flemish Cap on the Newfoundland rifted margin, *Geology*, in press, 2003.

Jokat, W., O. Ritzmann, M. C. Schmidt-Aursch, S. Drachev, S. Gauger, and J. Snow, Geophysical evidence for reduced melt production on the Arctic ultraslow Gakkel mid-ocean ridge, *Nature*, 423, 962–965, doi:10.1038/nature01706, 2003.

Keen, C. E., and D. L. Barrett, Thinned and subsided continental crust on the rifted margin of eastern Canada: Crustal structure, thermal evolution and subsidence history, *Geophys. J. R. Astron. Soc.*, 65, 443–465, 1981.

Keen, C. E., R. Boutilier, B. de Voogd, B. Mudford, and M. E. Enachescu, Crustal geometry and extensional models for the Grand Banks, eastern Canada: Constraints from deep seismic reflection data, in *Sedimentary Basins and Basin-Forming Mechanisms*, edited by C. Beaumont and A. J. Tankard, *Mem. Can. Soc. Pet. Geol.*, 12, 101–115, 1987.

Keen, C. E., C. Peddy, B. de Voogd, and D. Matthews, Conjugate margins of Canada and Europe: Results from deep reflection profiling, *Geology*, 17, 173–176, 1989.

Kent, D. V., and F. M. Gradstein, A Jurassic to recent chronology, in *The Geology of North America*, vol. M, *The Western North Atlantic Region*, edited by P. R. Vogt and B. E. Tucholke, pp. 45–50, Geol. Soc. of Am., Boulder, Colo., 1986.

King, L. H., G. B. Fader, W. H. Poole, and R. K. Wanless, Geological setting and age of the Flemish Cap granodiorite, east of the Grand Banks of Newfoundland, *Can. J. Earth Sci.*, 22, 1286–1298, 1985.

Klingelhöfer, F., L. Géli, L. Matias, N. Steinsland, and J. Mohr, Crustal structure of a super-slow spreading centre: A seismic refraction study of Mohns Ridge, 72°N, *Geophys. J. Int.*, 141, 509–526, 2000.

Louden, K. E., and D. Chian, The deep structure of non-volcanic rifted continental margins, *Philos. Trans. R. Soc. London, Ser. A*, 357, 767–804, 1999.

Louden, K. E., and H. Lau, Insights from scientific drilling on rifted continental margins, *Geosci. Can.*, 28, 187–195, 2001.

Ludwig, W. J., J. E. Nafe, and C. L. Drake, Seismic refraction, in *The Sea*, edited by A. E. Maxwell, pp. 53–84, Wiley-Intersci., Hoboken, N. J., 1970.

Lutter, W. J., and R. L. Nowack, Inversion for crustal structure using reflections from the PASSCAL Ouachita experiment, *J. Geophys. Res.*, *95*, 4633–4646, 1990.

Marillier, F., et al., Lithoprobe East onshore-offshore seismic refraction survey - constraints on interpretation of reflection data in the Newfoundland Appalachians, *Tectonophysics*, *232*, 43–58, 1994.

Mauffret, A., and L. Montadert, Rift tectonics on the passive continental margin off Galicia (Spain), *Mar. Pet. Geol.*, *4*, 49–70, 1987.

Miller, D. J., and N. I. Christensen, Seismic velocities of lower crustal and upper mantle rocks from the slow-spreading Mid-Atlantic Ridge, south of the Kane Transform zone (MARK), *Proc. Ocean Drill. Program Sci. Results*, *153*, 437–454, 1997.

Minshull, T. A., S. M. Dean, R. S. White, and R. B. Whitmarsh, Anomalous melt production after continental break-up in the southern Iberia Abyssal Plain, in *Non Volcanic Rifting of Continental Margins*: *A Comparison of Evidence From Land and Sea*, edited by R. C. L. Wilson et al., *Geol. Soc. Spec. Publ.*, *187*, 537–550, 2001.

Murillas, J., D. Mougenot, G. Boillot, M. C. Comas, E. Banda, and A. Mauffret, Structure and evolution of the Galicia Interior Basin (Atlantic western Iberian continental margin), *Tectonophysics*, *184*, 297–319, 1990.

Mutter, C. Z., and J. C. Mutter, Variations in thickness of layer 3 dominate oceanic crustal structure, *Earth Planet. Sci. Lett.*, *117*, 295–317, 1993.

Pérez-Gussinyé, M., and T. J. Reston, Rheological evolution during extension at nonvolcanic rifted margins: Onset of serpentinization and development of detachments leading to continental breakup, *J. Geophys. Res.*, *106*, 3961–3975, 2001.

Pérez-Gussinyé, M., T. J. Reston, and J. Phipps Morgan, Serpentinization and magmatism during extension at non-volcanic margins: The effect of initial lithospheric structure, in *Non Volcanic Rifting of Continental Margins*: *A Comparison of Evidence From Land and Sea*, edited by R. C. L. Wilson et al., *Geol. Soc. Spec. Publ.*, *187*, 551–576, 2001.

Pérez-Gussinyé, M., C. R. Ranero, T. J. Reston, and D. Sawyer, Structure and mechanisms of extension at the Galicia Interior Basin, west of Iberia, *J. Geophys. Res.*, *108*(B5), 2245, doi:10.1029/2001JB000901, 2003.

Pickup, S. L. B., R. B. Whitmarsh, C. M. R. Fowler, and T. J. Reston, Insight into the nature of the ocean-continent transition off west Iberia from a deep multichannel seismic reflection profile, *Geology*, *24*, 1079–1082, 1996.

Pinheiro, L. M., R. B. Whitmarsh, and P. R. Miles, The ocean-continent boundary off the western continental margin of Iberia-II. Crustal structure in the Tagus Abyssal Plain, *Geophys. J. Int.*, *109*, 106–124, 1992.

Reid, I., Crustal structure of a nonvolcanic rifted margin east of Newfoundland, *J. Geophys. Res.*, *99*, 15,161–15,180, 1994.

Reid, I. D., and C. E. Keen, High seismic velocities associated with reflections from within the lower oceanic crust near the continental margin of eastern Canada, *Earth Planet. Sci. Lett.*, *99*, 118–126, 1990.

Reston, T. J., C. M. Krawczyk, and D. Klaeschen, The S reflector west of Galicia (Spain): Evidence from prestack depth migration for detachment faulting during continental breakup, *J. Geophys. Res.*, *101*, 8075–8091, 1996.

Sandwell, D. T., and W. H. F. Smith, Marine gravity anomaly from Geosat and ERS 1 satellite altimetry, *J. Geophys. Res.*, *102*, 10,039–10,054, 1997.

Sawyer, D. S., R. B. Whitmarsh, A. Klaus, and Shipboard Scientific Party, *Proceedings of the Ocean Drilling Program, Initial Reports*, vol. 149, 719 pp., Ocean Drill. Program, College Station, Tex., 1994.

Srivastava, S. P., J. Verhoef, and R. Macnab, Results from a detailed aeromagnetic survey across the northeast Newfoundland margin, Part II: Early opening of the North Atlantic between the British Isles and Newfoundland, *Mar. Pet. Geol.*, *5*, 324–337, 1988.

Srivastava, S. P., J.-C. Sibuet, S. Cande, W. R. Roest, and I. D. Reid, Magnetic evidence for slow seafloor spreading during the formation of the Newfoundland and Iberian margins, *Earth Planet. Sci. Lett.*, *182*, 61–76, 2000.

Talwani, M., J. L. Worzel, and M. Landisman, Rapid gravity computations for two-dimensional bodies with application to the Mendocino submarine fracture zone, *J. Geophys. Res.*, *64*, 49–59, 1959.

Tankard, A. J., and H. J. Welsink, Mesozoic extension and styles of basin formation in Atlantic Canada, *AAPG Bull.*, *71*, 1210–1232, 1987.

Todd, B. J., and I. Reid, The continent-ocean boundary south of Flemish Cap: Constraints from seismic refraction and gravity, *Can. J. Earth Sci.*, *26*, 1392–1407, 1989.

Tucholke, B. E., J. A. Austin Jr., and E. Uchupi, Crustal structure and rift-drift evolution of the Newfoundland Basin, in *Extensional Tectonics and Stratigraphy of the North Atlantic Margins*, edited by A. J. Tankard and H. R. Balkwill, *AAPG Mem.*, *46*, 247–263, 1989.

Verhoef, J., W. R. Roest, and R. Macnab, J. Arkani-Hamed, and Project Team, Magnetic anomalies of the Arctic and North Atlantic Oceans and adjacent land areas, *Geol. Surv. Can. Open File Rep.*, *3125a*, 1996.

White, R. S., D. McKenzie, and R. K. O'Nions, Oceanic crustal thickness from seismic measurements and rare earth element inversions, *J. Geophys. Res.*, *97*, 19,683–19,715, 1992.

Whitmarsh, R. B., L. M. Pinheiro, P. R. Miles, M. Recq, and J.-C. Sibuet, Thin crust at the Western Iberia ocean-continent transition and ophiolites, *Tectonics*, *12*, 1230–1239, 1993.

Whitmarsh, R. B., R. S. White, S. J. Horsefield, J.-C. Sibuet, M. Recq, and V. Louvel, The ocean-continent boundary off the western continental margin of Iberia: Crustal structure west of Galicia Bank, *J. Geophys. Res.*, *101*, 28,291–28,314, 1996.

Whitmarsh, R. B., M.-O. Beslier, P. J. Wallace, and Shipboard Scientific Party, *Proceedings of the Ocean Drilling Program, Initial Reports*, vol. 173, 493 pp., Ocean Drill. Program, College Station, Tex., 2000.

Zelt, C. A., Modelling strategies and model assessment for wide-angle seismic traveltime data, *Geophys. J. Int.*, *139*, 183–204, 1999.

Zelt, C. A., and D. A. Forsyth, Modeling wide-angle seismic data for crustal structure: Southeastern Grenville Province, *J. Geophys. Res.*, *99*, 11,687–11,704, 1994.

Zelt, C. A., and R. B. Smith, Seismic traveltime inversion for 2-D crustal velocity structure, *Geophys. J. Int.*, *108*, 16–34, 1992.

Zelt, C. A., A. Sain, J. V. Naumenko, and D. S. Sawyer, Assessment of crustal velocity models using seismic refraction and reflection tomography, *Geophys. J. Int.*, *153*, 609–626, doi:10.1046/j.1365-246X.2003.01919, 2003.

———————————

T. Funck, J. R. Hopper, and H. C. Larsen, Danish Lithosphere Centre, Øster Voldgade 10, L, 1350 Copenhagen K, Denmark. (tf@dlc.ku.dk)

K. E. Louden, Department of Oceanography, Dalhousie University, Halifax, Nova Scotia, Canada B3H 4J1. (keith.louden@dal.ca)

B. E. Tucholke, Department of Geology and Geophysics, Woods Hole Oceanographic Institution, Woods Hole, MA 02543-1541, USA. (btucholke@whoi.edu)

W. S. Holbrook, Department of Geology and Geophysics, University of Wyoming, Laramie, WY 82071-3006, USA. (steveh@uwyo.edu)